

AMERICAN UNIVERSITY OF BEIRUT

STRENGTHENING UNREINFORCED MASONRY
WALLS AGAINST OUT-OF-PLANE LOADING
USING HEMP FIBERS

by
REEM BASSAM BITAR

A thesis
submitted in partial fulfillment of the requirements
for the degree of Master of Engineering
to the Department of Civil and Environmental Engineering
of the Faculty of Engineering and Architecture
at the American University of Beirut

Beirut, Lebanon
March 2017

AMERICAN UNIVERSITY OF BEIRUT

STRENGTHENING UNREINFORCED MASONRY
WALLS AGAINST OUT-OF-PLANE LOADING
USING HEMP FIBERS

by
REEM BASSAM BITAR

Approved by:



Dr. George Saad, Assistant Professor
Department of Civil and Environmental Engineering

Advisor



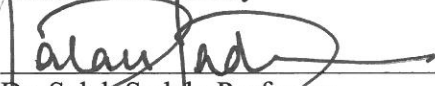
Dr. Mounir Mabsout, Chairperson
Department of Civil and Environmental Engineering

Co-Advisor



Dr. Elie Awwad, Associate Professor
Lebanese University

Member of Committee



Dr. Salah Sadek, Professor
Department of Civil and Environmental Engineering

Member of Committee

March 22, 2017

AMERICAN UNIVERSITY OF BEIRUT

THESIS, DISSERTATION, PROJECT RELEASE FORM

Student Name:

Bassam Bitar Reem
Middle Last First

Master's Thesis Master's Project Doctoral Dissertation

I authorize the American University of Beirut to: (a) reproduce hard or electronic copies of my thesis, dissertation, or project; (b) include such copies in the archives and digital repositories of the University; and (c) make freely available such copies to third parties for research or educational purposes.

I authorize the American University of Beirut, to: (a) reproduce hard or electronic copies of it; (b) include such copies in the archives and digital repositories of the University; and (c) make freely available such copies to third parties for research or educational purposes after:

One ~~---~~ year from the date of submission of my thesis, dissertation, or project.
Two ---- years from the date of submission of my thesis, dissertation, or project.
Three ---- years from the date of submission of my thesis, dissertation, or project.

Reem Bitar April 12, 2017
Signature Date

ACKNOWLEDGMENTS

I would like to express my deepest gratitude and appreciation to my advisor Dr. George Saad for his continuous supervision, advice, and support. I would like to also thank Dr. Elie Awwad for his help in finding valuable resources and Dr. Mounir Mabsout for his encouragement and support throughout the research.

Many thanks to Mr. Helmi Khatib, Civil and Environmental Engineering Laboratories Manager, and Ms. Dima Hassanieh, Lab Engineer, for their endless support in my entire experimental work. I am also thankful to all the Civil and Engineering Laboratory staff, Mr. Abdul Rahman Al sheikh and Mr. Bashir Asyala for their valuable assistance.

I also appreciate the help and assistance of Mrs. Zakeya Deeb – Civil and Environmental Engineering Department Assistant, Mr. Khaled Noubani – Engineering librarian, Mr. Hisham Ghalayini – Mechanical Engineering Laboratories, and Mr. Joseph Nassif – Engineering Shop Supervisor.

I would like to thank my colleagues Ms. Riham Ramadan and Ms. Lea Ghalieh for their assistance.

AN ABSTRACT OF THE THESIS OF

Reem Bassam Bitar for Master of Engineering
Major: Civil Engineering

Title: Strengthening Unreinforced Masonry Walls against Out-of-plane Loading Using Hemp Fibers

Strengthening concrete masonry structures with fiber reinforced polymers is a method widely used for strengthening and rehabilitation purposes. Research on strengthening of masonry walls has been limited to the use of composites made from synthetic material such as carbon, glass or aramid fibers, etc. The existing knowledge in improving structures, including masonry walls, using natural fibers, is hardly applied. The replacement of synthetic fibers used as external reinforcement (carbon, glass and aramid) with natural fibers is a step to achieve a sustainable construction.

The objective of this study is to investigate the out-of-plane flexural behavior of unreinforced masonry walls strengthened with externally applied natural hemp fiber fabric. The test parameters investigated were the amount of hemp reinforcement layers and anchoring of the hemp reinforcement. In this study, unstrengthened and hemp-strengthened masonry wall specimens were tested in the out-of-plane direction.

The load-deflection curves, structural ductility measured by fracture energy and failure modes were analyzed. The ultimate moment capacity of the unstrengthened walls was estimated using a simple analytical approach. A proposed analytical model was used to determine the out-of-plane capacity of the hemp-strengthened walls. Results showed that externally bonded hemp fiber fabric composite systems significantly enhance the load carrying capacity and deflection capacity of unreinforced masonry walls subjected to out-of-plane loads. As the hemp reinforcement ratio increases, the flexural capacity and ductility of the walls also increase. The predicted ultimate load carrying capacities of strengthened and unstrengthened walls were considered conservative compared to experimental results.

CONTENTS

	Page
ACKNOWLEDGMENTS	v
ABSTRACT.....	vi
FIGURES.....	x
TABLES.....	xiii
 Chapter	
1. INTRODUCTION.....	1
1.1. Introduction.....	1
1.2. Objectives and Scope.....	3
1.3. Thesis Outline.....	4
2. BACKGROUND AND LITERATURE REVIEW.....	5
2.1. Introduction.....	5
2.2. Application of Natural Fibers as a Retrofitting Material.....	6
2.3. Retrofitting Masonry Walls.....	8
2.3.1. Synthetic Masonry Retrofitting Materials.....	8
2.3.2. Natural Fibers Masonry Retrofitting Materials.....	12
2.4. Hemp Fibers.....	14
2.4.1. Hemp Fiber Surface Modification.....	16

3.3.4.2. Hemp-Strengthened Walls.....	51
3.3.4.2.1. Proposed Methodology.....	51
3.3.5. Testing Program.....	54
3.3.5.1. Test Setup.....	54
3.3.5.2. Instrumentation.....	55
3.3.5.3. Test Procedure.....	56
4. DISCUSSION OF TEST RESULTS AND ANALYSIS.....	58
4.1. Introduction.....	58
4.2. Load – Deflection Behavior.....	58
4.3. Performance of Strengthened Walls.....	67
4.3.1. Flexural Strength Capacity.....	67
4.3.2. Ductility Index.....	68
4.4. Failure Modes.....	71
4.5. Performance of Analytical Model.....	80
4.5.1. Unstrengthened Walls.....	80
4.5.2. Hemp-Strengthened Walls.....	81
5. SUMMARY, CONCLUSIONS, AND RECOMMENDATIONS.....	83
5.1. Research Summary.....	83
5.2. Research Conclusions.....	84
5.3. Research Recommendations.....	86
REFERENCES.....	87

FIGURES

Figure	Page
3.1. Hemp Fiber Rope.....	20
3.2. Schematic Diagram of the Hemp Fiber Sample.....	21
3.3. Hemp Fiber Rope Tensile Test Setup.....	22
3.4. Control (Left) and Hemp-Confined (Right) Specimens.....	24
3.5. Test Setup for Compression Test of a Control Specimen (Left), and a Hemp Specimen (Right).....	25
3.6. Stress-Strain Curves for the Preliminary Study.....	26
3.7. C Type Test Specimens (Left), E Type Test Specimens (Right).....	28
3.8. H1 Type Test Specimens (Left), G Type Test Specimens (Right).....	28
3.9. Tensile Test Setup of Hemp Fabrics.....	31
3.10. Stress-Strain Curve of Hemp Fiber Fabrics.....	31
3.11. Individual Concrete Masonry Unit.....	33
3.12. Mortar Cubes.....	34
3.13. Crushed Mortar Cube.....	35
3.14. Masonry Prism.....	37
3.15. Strengthened Test Wall Specimens.....	39
3.16. Details of Test Walls: (a) Series Control; (b) Series H S; (c) Series H 1; (d) Series H 2; (e) Series H 3.....	41
3.17. Mason Laying First and Second Course of CMU.....	42
3.18. Mason Leveling the Walls.....	43

3.19.	Fully Constructed Masonry Walls.....	44
3.20.	Surface Preparation for Hemp Fiber Fabric Installation.....	44
3.21.	Cutting Hemp Fiber Fabric into Desired Width and Length.....	45
3.22.	Application of Primer prior to Hemp Fiber Fabric Installation.....	46
3.23.	Installation of Hemp Fabric to Masonry Wall (Series H1, H2, and H3).....	47
3.24.	Application of Hemp Fabric to Masonry Wall (Series HS).....	48
3.25.	Application of Anchors at the End of a Masonry Wall.....	49
3.26.	Internal Strain and Stress Distribution for a Typical URM Wall Section Strengthened with Hemp Fiber Fabric.....	52
3.27.	Test Setup and Dimensions of the Wall Specimens.....	54
3.28.	Wall Support.....	55
3.29.	Instrumentation Layout.....	56
3.30.	Positioning Wall Specimen into MTS Machine.....	57
3.31.	Test Setup of the Walls.....	57
4.1.	Load-Midspan Deflection Response for Control Wall C1.....	59
4.2.	Wall H S-b Load-Deflection Response.....	59
4.3.	Wall H 1-b Load-Deflection Response.....	60
4.4.	Wall H 1-b Load-Deflection Response.....	61
4.5.	Wall H 2-a Load-Deflection Response.....	61
4.6.	Wall H 2-b Load-Deflection Response.....	62
4.7.	Wall H 3-a Load-Deflection Response.....	62
4.8.	Wall H 3-b Load-Deflection Response.....	63
4.9.	Comparison of Load-Midspan Deflection Response of All Series.....	63

4.10.	Wall Deflections along the Length at P= 2 kN.....	64
4.11.	Wall Deflections along the Length at P= 4 kN.....	65
4.12.	Wall Deflections along the Length at P= 6 kN.	65
4.13.	Wall Deflections along the Length at P= 10 kN.....	66
4.14.	Maximum Wall Deflection at Ultimate Loads.....	66
4.15.	Gain in Out-of-Plane Capacity of Strengthened Walls.....	68
4.16.	Effect of Hemp Reinforcement Ratio on the Ductility Index.....	71
4.17.	Failure Mode of Control Wall C1.....	71
4.18.	Failure Mode of H1-a.....	72
4.19.	Failure Mode of H1-a (vertical view).....	73
4.20.	Failure Mode of H1-b.....	73
4.21.	Failure Mode of H1-b (vertical view).....	74
4.22.	Failure Mode of H2-a.....	74
4.23.	Failure Mode of H2-a (vertical view).....	75
4.24.	Failure Mode of H2-b.....	75
4.25.	Failure Mode of H2-b (vertical view).....	76
4.26.	Failure Mode of H3-a.....	77
4.27.	Failure Mode of H3-b.....	78
4.28.	Deflected Shape of Wall H3-b.....	79
4.29.	Schematic View of Series H3 Cracked Wall Specimen.....	79
4.30.	Failure Mode of HS-b.....	79
4.31.	Failure Mode of HS-b (vertical view).....	80
4.32.	Experimental Failure Load to Predicted Load Results.....	82

TABLES

Table		Page
2.1.	Typical Physical and Mechanical Properties of Hemp Fiber.....	15
2.2.	Tensile Properties of Hemp Fibers by Different Authors.....	16
3.1.	Key Testing Points per ASTM D 3822-14 (Symington et al., 2009).....	21
3.2.	Concrete Cylinder Test Matrix.....	23
3.3.	Mechanical Properties of Epoxy Resin Sikadur 300.....	32
3.4.	Results of Masonry Unit Compression Test.....	33
3.5.	Results of Mortar Cube Test.....	35
3.6.	Results of Prism Test.....	37
3.7.	Masonry Walls Testing Matrix.....	39
3.8.	Test Matrix Details.....	40
4.1.	Fracture Energy and Ductility Index of the Wall Specimens.....	70
4.2.	Summary of Experimental Results for Walls Tested in this Study.....	72
4.3.	Experimental and Analytical Results for Unstrengthened Wall.....	81
4.4.	Experimental and Analytical Results for Hemp Strengthened Walls.....	82

To My Beloved Family

CHAPTER 1

INTRODUCTION

1.1. Introduction

A large percentage of existing buildings around the world have been constructed with unreinforced masonry. Unreinforced masonry buildings (URM buildings) are threatened to collapse during earthquakes, which imposes high safety risks. Damage or collapse of unreinforced masonry buildings is dangerous not only to their occupants but also to pedestrians and to those in adjacent buildings. Even if the entire building does not collapse, falling masonry debris is potentially lethal. Thus, there is an urgent need to strengthen unreinforced masonry buildings.

Retrofitting is considered a seismic risk reduction technique to strengthen URM buildings. It is a process of adding seismic resistance to an existing building. Common retrofitting materials include glass and carbon fiber-reinforced polymers (GFRP and CFRP) which enhance both flexural and shear capacity of masonry walls (Pampanin, 2006). FRP is applied in thin films to the exterior surface of walls painted with a layer of epoxy. The tensile strength of the mortar, which is very small in most aging structures, limits the flexural strength of URM walls. When GFRP or CFRP is bonded to the exterior surface of the wall, it provides a large tensile component that, along with the compressive strength of the masonry, can resist large flexural load.

Structural strengthening of an URM building is a significant construction project. It imposes high cost that may affect owners, occupants, and community at large (Reitherman & Perry, 2009); thus, finding cheaper alternatives would be beneficial. Until

recently, retrofitting jobs of structures have been limited to the use of carbon, glass or aramid fibers, etc. The existing knowledge in improving structures using naturally available materials, or natural fibers, is hardly applied. This is due to the need to expand this knowledge and study more the effect and durability of natural fibers in structural application. The strengthening of structural facilities with the application of composites is due to the help of artificial fibers that make up the composites, and the issue of sustainability of these raw materials used for strengthening purposes is not addressed. The use of raw natural fibers for structural strengthening would make use of locally available materials, exploit local skills, reduces waste material, benefits local economy by being income generating, and is low in monetary cost (Shahzad, 2011).

Recent research proved that using natural fibers in construction reinforcement results in acceptable strength improvement (Menna et al., 2015). Natural fibers are highly available and this encouraged the development of plant fiber composites. Among the various natural fibers such as, sisal, bamboo, coir, and jute fibers, hemp fibers are of particular interest as these fibers have high impact strength as well as good tensile and flexural properties compared to other lignocellulosic fibers. Their mechanical properties are comparable to those of glass fiber; this makes them a suitable material to replace glass fibers as reinforcements in composite materials (Shahzad, 2011). Hemp is abundant in nature, does not require intensive care to grow, and is a waste material most of the time (Sen & Reddy, 2011). Thus, with further research, hemp fibers may be used as an alternative to FRP in retrofitting URM buildings.

1.2. Objectives and Scope

The broad objective of the research is to investigate the out-of-plane flexural behavior of unreinforced masonry walls strengthened with externally applied natural hemp fiber fabric. Emphasis is placed on the load-deflection response of the wall specimens tested. Since little information exists on externally applied natural hemp fiber fabric on masonry walls, an attempt is made to explain the overall behavior of the wall specimens including crack patterns, and the interaction between the hemp fiber fabric and the masonry.

To achieve these objectives, a total of ten concrete masonry walls were built of which eight walls were retrofitted with hemp fiber fabric of different configurations. The walls were tested as simply supported beams subjected to two out-of-plane line loads which produced a constant moment region between the loading lines where the primary data were collected. The load-deflection response of masonry walls strengthened with hemp fiber fabric systems when subjected to transverse or out-of-plane loads was determined from static laboratory tests. The performance of the used strengthening technique was determined by examining strength, stiffness, ductility, and failure modes of the wall specimens. The ultimate moment capacity of the unstrengthened walls was estimated using a simple analytical approach and results were compared with the moment capacity calculated according to the Masonry Standard Joint Committee (MSJC 2013) code specifications for masonry structures. A proposed analytical model was used to determine the out-of-plane capacity of the hemp-strengthened walls and results were compared to the experimental results.

1.3. Thesis Outline

This thesis is divided into five chapters. Chapter 1 is an introduction and background on the topic of strengthening masonry elements of buildings and the use of natural fibers, and a summary of the research objective and scope. Chapter 2 presents background and a review of the current literature on strengthening masonry walls against out-of-plane loading and natural fibers as a strengthening material. The details of the experimental program and testing methodology are presented in Chapter 3. Chapter 4 summarizes and discusses the results of the experimental program conducted. The load-deflection behavior of the specimens is analyzed and the failure modes are described. Chapter 5 summarizes and concludes the research and includes further research recommendations.

CHAPTER 2

BACKGROUND AND LITERATURE REVIEW

2.1. Introduction

Composite materials from synthetic fibers (i.e. glass fiber, carbon fiber etc.) are already available as products for consumer and industrial uses. A relatively newer concept, driven by consumer environmental awareness, is to consider natural fibers, a renewable material independent of fossil fuels, as a reinforcing material (Sen & Reddy, 2011). In recent years, strengthening of reinforced concrete (RC) structures using fiber-reinforced polymers (FRP) has become very popular in the construction industry (Abdo & Hori, 2012). Currently, the main reinforcement for the composite industry is glass fibers; 22.3 million tons are produced globally on an annual basis. High energy is consumed for the manufacturing of these products; also there is no recycling option at the end of their life cycle. Considering the alternative, annual industrial crops grown for fiber have the potential to supply enough renewable biomass for various bioproducts including composites.

In many developing countries where natural fibers are abundant, economic factors require the utilization of these natural fibers as effectively and economically as possible for structural strengthening and also for various other applications in civil engineering (Sen & Reddy, 2011). Approximately, 43,000 tons of natural fibers were used as reinforcement materials in FRP composites in EU in 2003 (Liu et al., 2007). Growth in development of natural fibers increased this amount to around 315,000 tons in 2010, which accounted for 13% of the total reinforcement materials (glass, carbon

and natural fibers) in FRP composites. Estimations present that about 830,000 tons of bio-fibers will be consumed by 2020 and the share will go up to 28% of the total reinforcement materials (Carus & ScholZ, 2011).

2.2. Application of Natural Fibers as a Retrofitting Material

This section presents a review of various studies that investigate the application of different natural fibers as reinforcing material for structural upgrading. Following this section, a review of retrofitting masonry walls is presented.

Sen T. and Reddy H. (2011) studied numerically the flexural stiffness of both: beams retrofitted with Bamboo fiber reinforced composites and beams retrofitted with Coir fiber reinforced composites. They concluded that the FRP was found to be effective only after the initial cracking of concrete and by providing different percentages of Bamboo fibers or Coir fibers for retrofitting, the load carrying capacity of reinforced concrete beam models can be enhanced as compared to that of the controlled specimens. Most recently, Yan et al. (2012, 2013, and 2014) used inexpensive natural flax fiber to compose flax FRP (FFRP) tube to confine coir fiber reinforced concrete. The combined studies revealed that in axial compression, FFRP tube confinement enhances the compressive strength and ductility of both plain concrete (PC) and coir fiber reinforced concrete (CFRC) significantly and this enhancement increases with an increase in tube thickness. Compression test results showed that the failure mode of flax FRP confined concrete was dominated by the rupture of flax FRP in the hoop directly when the hoop tensile strength exceeds the tensile strength of FFRP tube. The results indicate that natural FRP composites as concrete confinement can increase the compressive and flexural properties of concrete. The compressive behavior

of FRP tube confined concrete is significantly influenced by the unconfined concrete compressive strength as reported by Li et al. (2005). The confinement performance of FRP tube on low strength concrete is significantly larger than that on high strength concrete (Li et al., 2005).

One alternative to FRP may be using fiber-reinforced mortars (FRM) for structural upgrading, but it would be inhibited by the relatively poor bond conditions in the cementitious composite due to the poor penetration of mortar in fiber sheets. If continuous fiber sheets were replaced by textiles, this would result in a new generation of materials, textile-reinforced mortars (TRM) that enhance fiber-matrix interactions. This new material may substitute FRP in the field of strengthening and seismic retrofitting (Papanicolaou, Triantafillou, & Lekka, 2011). The effectiveness of the TRM technique for reinforced concrete (RC) elements has been experimentally investigated by Triantafillou and Papanicolaou (2006), Triantafillou et al. (2006) and Bournas and Triantafillou (2009), and has been extended to masonry structures by Papanicolaou et al. (2007 and 2008) and Prota et al. (2006). Papanicolaou et al. (2007 and 2008) studied experimentally the application of textile-reinforced mortar (TRM) as a means of increasing the load carrying capacity and deformability of unreinforced masonry walls (URM) subjected to cyclic in-plane loading. Results show that TRMs comprise a promising solution for the structural rehabilitation of masonry structures under in-plane loading and for increasing the confinement and shear capacity of RC members.

2.3. Retrofitting Masonry Walls

2.3.1. Synthetic Masonry Retrofitting Materials

Several investigations (Saadatmanesh 1994 and 1997, Ehsani 1995, Eshani and Saadatmanesh 1997, and Michael et al. 2001) have indicated that the out-of-plane strength and ductility of unreinforced masonry walls may be enhanced by externally bonded FRP reinforcement. Tan and Patoary (2004) studied the response of thirty masonry walls strengthened using three different fiber-reinforced polymer (FRP) systems, with three anchorage methods. The walls were fabricated and tested under a concentrated load over a 100 mm square area or a patch load over a 500 mm square area. The test results indicated a significant increase in the out-of-plane wall strength over the un-strengthened wall. While failure occurred in the un-strengthened wall by bending, four different modes of failure, that is, punching shear through the bricks, debonding of FRP reinforcement from the masonry substrate, crushing of brick in compression, and tensile rupture of the FRP reinforcement, were observed in the strengthened walls. With appropriate surface preparation and anchorage systems, premature failure due to FRP debonding is prevented. It has also been found that the load-carrying capacity increased when the thickness of FRP laminates was increased. From the tests carried out, it can be concluded that the combination of surface grinding and fiber bolt anchorage system results in the greatest increase in wall strength. Bidirectional fiberglass woven fabrics could provide higher strength enhancement than carbon or glass fiber sheets if an appropriate adhesive is used. The test results compared well with the predictions of the proposed analytical models.

ElGawady et al. (2005) investigated in-plane seismic behavior of URM walls before and after retrofitting using fiber-reinforced polymers (FRP). Five walls were

dynamically tested as reference specimens. Then, these reference specimens were retrofitted on a single side using different types and structures of FRPs and retested. The FRP retrofitting technique is effective in significantly increasing the in-plane strength, stiffness, and deformability of URM walls. Simple linear elastic design approach predicted flexural strengths of the slender specimens on average 24% lower than their experimental strengths. Existing shear models predicted shear strengths ranging from 100 to 170% of the measured lateral strengths of the squat specimens. However, these specimens did not reach their ultimate strengths due to test set-up limitations.

Static-cyclic shear load tests and tensile tests on retrofitted masonry walls were conducted at UAS Fribourg by Bischof and Suter (2014) for an evaluation of a newly developed retrofitting system, the S&P ARMO-System which consists of a composite of carbon mesh embedded in a specially adapted high quality spray mortar. The experimental study has shown that masonry walls reinforced by this retrofitting system reach a similar strength and a higher ductility than retrofits by means of bonded carbon fiber reinforced polymer sheets. Hence, the retrofitting system using carbon fiber meshes embedded in a high quality mortar constitutes a good option for static or seismic retrofits or reinforcements for masonry walls.

Kalali and Kabir (2012) studied the in-plane behavior of one-half scale perforated brick walls with different Glass Fiber Reinforced Polymers (GFRPs) strengthening patterns under cyclic shear-compression loading in a quasi-static test facility. Each specimen was retrofitted on the surface of two sides. Strengthening by means of GFRPs significantly improved the strength, deformation capacity, and energy absorption of the brick wall. The increase in performance parameters was dependent upon GFRP layout. The cross configuration for GFRP is more efficient in terms of the

in-plane load bearing capacity of a strengthened brick wall than the grid configuration; because only the former is effective against entire failure mechanisms in brick walls. The original failure mode of the perforated unreinforced brick walls clearly changed from shear to other failure modes, such as sliding mode, rocking mode, and mixed failure modes, due to GFRP strengthening. Consequently, substantial gains in in-plane strength were achieved up to the threshold of the values corresponding to the capacity of these new failure modes.

Hamoush et al. (2001) investigated the effectiveness of using fiber-reinforced composite overlays of two configurations ((A) web and (B) vertical and horizontal bands of unidirectional fiber composites) to strengthen existing unreinforced masonry walls to resist out-of-plane static loads. In addition to the two fiber configurations, the testing program also evaluated two methods of surface preparation of the walls, sand blasting, and wire brush. It has been concluded that strengthening of unreinforced masonry walls by externally bonded composite overlays increases the flexural strength. However, the ultimate flexural strength is not achievable unless the premature failure by shear at the support is controlled. Most of the tested walls failed by shear at the end connection of the fiber system with the masonry walls. In comparison to any other surface preparation technique, sand blasting or manual steel brush cleaning produced sufficient bond at the interface between the fiber and the CMU blocks for both fiber configurations. Also retrofitting of masonry wall systems by a continuous web overlay on the entire wall area (pattern A) produced a slightly higher strength than walls retrofitted by the unidirectional strips applied in two directions (pattern B).

Masonry walls strengthened with FRP can have large increase in strength, but the effect of the presence of damage in the walls at the time of the repair has not been

studied. Santa-Maria and Alcaino (2011) studied the performance of clay brick masonry walls that were initially damaged in shear by loading them up to their maximum strength, then were repaired using two configurations of externally bonded carbon fiber strips and tested under cyclic shear loading up to failure. It was observed that the maximum strength and deformation capacity, as well as the cracking pattern and failure mode, of the repaired walls was similar to that of undamaged walls that were strengthened with the same reinforcing schemes of CFRP.

Papanicolaou et al. (2007, 2008) evaluated the effectiveness of Textile Reinforced Mortar (TRM) overlays in comparison to effectiveness of FRPs against in-plane and out-of-plane cyclic loading. The parameters under investigation included the matrix material (mortar versus resin), the number of textile layers and the compressive stress level applied to shear walls and beam-columns. Compared with their resin-impregnated counterparts, mortar-impregnated textiles may result in generally lower effectiveness in terms of strength, but in much higher in terms of deformability. TRM jackets were at least 65–70% as effective as FRP jackets with identical fiber configurations. In terms of deformability, of crucial importance in seismic retrofitting of unreinforced masonry walls, TRM jacketing is much more effective than FRP. Moreover, regardless of the matrix material (mortar versus resin), the strength generally increases with the number of layers and the axial load, at the expense of deformability. It has been observed that if failure is controlled by damage in the masonry, TRM overlays outperform their FRP counterparts based on maximum load and displacement at failure, whereas if the failure mechanism involves tensile fracture of the textile reinforcement the effectiveness of TRM versus FRP is slightly reduced. From the

results obtained in this study it is believed that TRMs hold strong promise as a solution for the structural upgrading of masonry structures under in-plane loading.

Anil et al. (2012) performed an experimental study for improving the out-of-plane strength of URM brick walls. CFRP materials were used for strengthening wall specimens and the variables examined in the study were CFRP strip layouts and usage of CFRP anchorages. They reported that the technique of strengthening with CFRP strips of different configurations increased the strength of the specimens 9 times, ductility ratio 3.5 times; energy dissipation capacity 125 times compared to URM masonry walls.

The efficiency of enhancing flexural capacity of URM walls in out-of-plane action using ferrocement overlay has been investigated by Kadam et al (2014). Six URM panels and 12 strengthened panels have been subjected to flexural strength test, parallel and perpendicular to bed-joints. The effect of strengthening on common parameters, pertaining to out-of-plane flexural behavior of ferrocement–URM composite walls, including failure modes, flexural strength, and modulus of rupture, have been investigated. The experimental results were compared with analytical results obtained using ordinary beam theory. The results showed that the URM panels exhibit sudden brittle failure whilst strengthened panels failed in a ductile fashion and exhibited a significant increase in the flexural strength. Further, the ordinary beam theory was able to predict the experimental results with reasonable accuracy.

2.3.2. Natural Fibers Masonry Retrofitting Materials

Most recently, Menna et al. (2015) investigated the shear behavior of masonry panels strengthened with a mortar-based system reinforced with an innovative hemp

fibre composite grid. The objective of the study was to assess the feasibility of using the proposed strengthening system for external retrofit of existing masonry walls and to compare its performances with typical retrofitting solutions. In this study, the in-plane response of strengthened NYT and clay masonry panels has been investigated. The strengthening system consisted of an innovative hemp fiber composite bi-directional grid externally bonded to each side of the panels by means of two different mortars, i.e. a pozzolanic and a NHL mortar. The strengthening system was conceived to pursue sustainable goals in construction industry and, specifically, to effectively employ natural fiber in structural retrofit/rehabilitation activities.

Twisted hemp yarns were impregnated in a flexible epoxy resin which allowed the exploitation of the good tensile properties of hemp fibers. The experimental outcomes, in terms of diagonal compression behavior, showed enhanced mechanical properties in all the investigated reinforced panels. The failure of the strengthened panels occurred with a mostly uniform crack pattern that developed along the loading direction. A clear ductile behavior, especially in case of pozzolanic based matrix system, was also exhibited by the strengthened panels, whereas the un-strengthened ones presented behavior a linear up to final failure. The investigated strengthening systems appear to exhibit good performances when compared with similar existing available/commercial solutions. The increase in the shear strength of the panels was similar to those attained by Balsamo et al. and Parisi et al. who tested similar NYT panels and strengthening solutions, employing glass and basalt FRP grids in lieu of the hemp grids here tested. Thus, given the interesting results herein achieved, authors believe that this system deserves further investigations, exploring different

configurations of the hemp composite system as well as confirming the validity of this system as seismic retrofit solution of masonry structures.

2.4. Hemp Fibers

Hemp is the most widely used natural fiber as reinforcement in composites. It is naturally one of the most ecologically friendly fibers and the oldest. A plant native to Central Asia, hemp is known to have been grown for more than 10,000 years. It is now grown mostly in the EU, Central Asia, Philippines, and China (Shahzad, 2011).

According to Food and Agriculture Organization (FAO), almost half of the world's industrial hemp supply is grown in China (2009).

In the hemp plant, fibers are contained within the tissues of the stems which help to hold the plant vertically. These fibers impart strength and stiffness to the tree. Hemp fibers' high strength and stiffness makes them a useful material to be used as reinforcement in composite materials. In recent years, the use of hemp for various applications has increased (Shahzad, 2011). According to FAO, world production of hemp fiber grew from 50,000 tons in 2000 to almost 90,000 tons in 2005.

Perhaps the most critical disadvantage of hemp fibers is the variability in their composition. This invariably results in variability in their physical and mechanical properties. Diameters and properties of natural fibers vary significantly depending upon many factors such as source, age, retting and separating techniques, geographic origin, rainfall during growth, and constituents' content (Netravali & Chabba, 2003). It is natural to expect that this variability in diameter will also impart variability to the mechanical properties of the fibers.

Nishino (2004) has identified the following factors that can cause the variability in the physical and mechanical properties of natural fibers: materials and measurement conditions. Materials such as (i) Microscopic: crystallinity, microfibril angle, and crystal modifications, (ii) Macroscopic: fineness, porosity, size, and shape of lumen, and (iii) History, source, age, retting and separating conditions, geographical origin, and rainfall during growth. Measurement conditions include tensile test speed, initial gauge length, moisture, temperature, and different cross-section of fibers at different points.

Table 2.1 Typical Physical and Mechanical Properties of Hemp Fiber (Shahzad, 2011).

Properties	Values
Diameter (ultimate) (μm)	17 – 23
Specific apparent density (gravity)	1500
Moisture content (%)	12
Cellulose content (%)	90
Tensile strength (MPa)	310 – 750
Specific tensile strength (MPa)	210 – 510
Young’s modulus (GPa)	30 – 60
Specific Young’s modulus (GPa)	20 – 41
Failure strain (%)	2 – 4

Catling (1982) measured the diameters of hemp fiber bundles and found the average to be 30 mm with a range of 11.68 - 31.96 mm. Olesen and Plackett (1999) found the average hemp fiber bundle diameter to be 25 mm. Table 2.1 shows typical physical and mechanical properties of hemp fiber and Table 2.2 shows tensile properties

of hemp fibers as reported by different authors. These values are representative values for these properties with considerable scope for variation (Shahzad, 2011).

Table 2.2 Tensile Properties of Hemp Fibers by Different Authors (Shahzad, 2011).

Tensile strength (MPa)	Tensile modulus (GPa)	Elongation at break (%)	Reference
690	NA	1.6	(Netravali & Chabba, 2003)
1235	NA	4.2	(Jarman, 1998)
310 – 750	30 – 60	2 – 4	(Ivens, Bos, & Verpoest, 1997)
550 – 900	70	1.6	(Brouwer, 2000)
690	NA	1.6	(Bledzki, Reihmane, & Gassan, 1996)
895	25	NA	(Bolton, 1995)
500 – 1040	32 – 70	1.6	(Mougin, 2006)
920	70	NA	(Berglund, 2006)
690 – 1000	50	1.0 – 1.6	(Mueller & Krobjilowski, 2003)
920	70	1.7	(Baucchio, 1994)
270 – 900	20 – 70	1.6	(Bogoeva-Gaceva et al., 2007)

2.4.1. Hemp Fiber Surface Modification

A strong degree of bonding is needed for effective transfer of stress from matrix to fibers in composite materials and this requires surface modification of fiber surfaces. A number of studies have been carried out on the effects of different fiber surface treatments on the properties of hemp fiber composites (Shahzad, 2011). In what follows, it is a brief review which shows that considerable improvements can be gained in the mechanical properties of hemp fiber composites by using the suitable surface treatment.

Wang et al. (2007) exposed hemp fibers of nano-scale (30–100nm width) to 12% NaOH solution. The cellulose content was found to increase significantly from 76% for untreated fibers to 94% for treated fibers. There was corresponding decrease in hemicelluloses of 10.7% for untreated fibers to 1.9% for treated fibers. X-ray

crystallography of fibers showed that the crystallinity of fibers increased after the treatment, thus affirming the increase in cellulose content. Beckermann and Pickering (2008) used 10% NaOH and 5% NaOH/2% Na₂SO₃ solutions for treatment of hemp fibers. NaOH treatment was more effective in removal of lignin and increased the crystallinity index of fibers following the treatment. The treated fibers were also more thermally stable than untreated fibers. Both the treatments resulted in increase in tensile properties of hemp-PP composites. It was also found that the tensile strength and stiffness increased with increase in the concentration of NaOH up to a limit (Shahzad, 2011).

Bledzki et al. (2004) used 22% NaOH solution on hemp fibers and studied the properties of unidirectional hemp yarn-epoxy composites. The flexural strength was increased by 45% and flexural modulus was increased by 100% following the treatment. Based on the literature review (Sedan et al., 2008). The natural fibers were treated and soaked in a sodium hydroxide solution (NaOH) at 6% by weight for 48 hours. After soaking, the fibers were washed with water and left to dry, and then separated using a mechanical tool. Trial concrete mixes have been tried with treated and untreated hemp fibers; however, the performance of the untreated fibers was not acceptable in terms of the bond with surrounding matrix, and thus the flexural performance did not improve compared to the plain mixes.

CHAPTER 3

EXPERIMENTAL PROGRAM

3.1. Introduction

The experimental program consisted of two parts. Part one consisted of preliminary testing of a total of twelve concrete cylinders 100 mm in diameter and 200 mm in height, six of which were confined with hemp natural rope fibers. The hemp-confined cylinders were all tested in compression and results were compared with the unconfined control specimens. Part two of the experimental program consisted of ten masonry walls 2,050 mm in length, 630 mm in width, and 100 mm in depth; the test matrix included two unreinforced walls and eight walls reinforced with hemp fiber bidirectional fabric sheets. The walls were subjected to a third-point loading in the out-of-plane direction by two line loads with the loading points $\ell_{span}/3$ from the reaction supports creating a constant moment region of $\ell_{span}/3$ long. The hemp fiber fabric reinforcement was installed on the tension side of the wall. The parameters investigated were the amount of reinforcement layers and anchorage of the hemp reinforcement. This chapter presents the materials, auxiliary material tests, as well as the test set-up and details of the specimens for part one and two of the experimental program.

3.2. Part One: Preliminary Testing

This section presents the first part of the experimental program. In this part, preliminary testing to study the effect of hemp rope confinement in strengthening concrete cylinders was conducted. The main objective of the preliminary testing is to

confirm the effectiveness of hemp as a reinforcement material that may substitute synthetic FRP. The following subsections present the materials used, testing specimens, and testing program that has been conducted followed by preliminary test results obtained.

3.2.1. Materials

3.2.1.1. Hemp Fibers

Raw long hemp fibers were used to conduct this study. The long fibers contained impurities and dust that affect the performance of these fibers and their interfacial bonding. Based on the literature, hemp fiber surface treatment improves fiber interfacial bonding as well as increases fiber mechanical properties (Symington et al. 2009). The hemp fiber surface treatment was adopted from Awwad et al. (2011) by soaking the long hemp fibers into 6% NaOH solution for 48 hours in room temperature conditions. Then the long fibers were washed by water several times to remove any excess NaOH, combed and sun dried.

Long ropes of hemp fibers were manually prepared to confine concrete cylinders for the study. Each rope was made of three single long hemp fibers that were twisted around each other to form a rope. The variability in the diameter of single hemp fibers resulted in varying diameter of ropes. This variability in rope diameters of hemp fibers affects the tensile strength of each rope. For this reason, the tensile strength property of hemp fiber was tested on ten samples of hemp ropes of specified length. Figure 3.1 shows a short segment of a prepared hemp fiber rope.



Figure 3.1 Hemp Fiber Rope.

3.2.1.1.1. Tensile Test

In order to conduct the tensile test for the hemp fiber ropes, ten variable samples from the previously prepared ropes were cut to a designated length of 100 mm. In each sample, the hemp fibers were fixed from both sides by cardboard with super glue to prevent the fibers from slipping off the tensile testing machine grips. The samples were allowed to cure for minimum 10 days before testing. Figure 3.2 shows a schematic of the hemp rope samples.

For the tensile testing of natural fiber, the closest applicable standard used was ASTM D 3822-14 the ‘Standard for Tensile Properties of Single Fibers’. This ASTM standard is typically used to quantify the mechanical properties of textile fibers and threads, which are often from a natural source, such as flax or cotton. This standard provides a good guideline as it is on the correct testing scale with the fibers being fine in cross-section. Table 3.1 highlights the key testing areas derived from the ASTM standard and discusses their importance in the testing procedure.

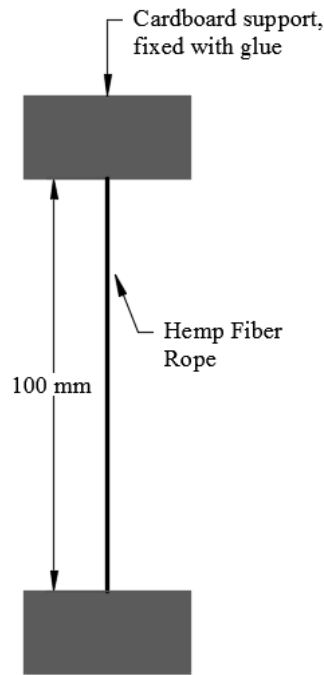


Figure 3.2 Schematic Diagram of the Hemp Fiber Sample.

Table 3.1 Key Testing Points per ASTM D 3822-14 (Symington et al., 2009).

Key Testing Area	Description
Constant rate of extension	The rate of extension of pull of the tensile testing machine has to be accurate and consistent for all the testing batches. In the testing for this study the rate of extension or pull was set 15 mm/min for all the fiber tests.
Fiber slippage in grips	The ASTM standard highlights the importance in preventing the slippage of the testing fiber through the fiber grips and therefore has to be avoided. Fiber slippage was carefully watched for during testing.
Fiber alignment	The alignment of the fibers in the jaws of the fiber grips has to be straight and square. This is to ensure that during testing the fiber is not being pulled at an angle to give distorted mechanical properties.
Gauge length	The gauge length is the distance between the edge of the upper and lower grips. This is the actual length of fiber being pulled during testing and it is important that this is kept constant throughout testing. The gauge length for testing was kept at 100 mm.

A general testing methodology was established for one individual fiber test.

Testing was then carried out 10 times to aid in accuracy of results and to indicate variations in values. Figure 3.3 shows a hemp rope sample being tested.

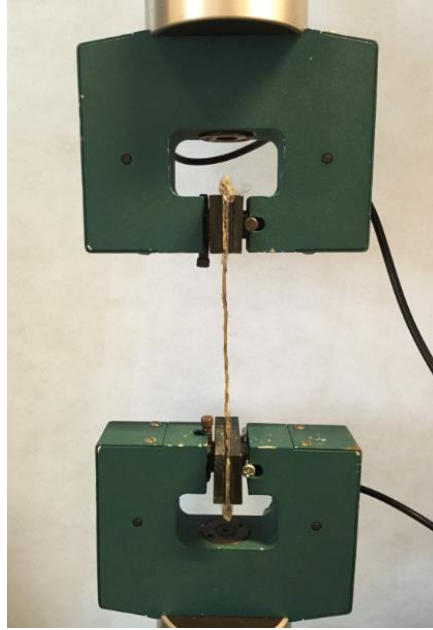


Figure 3.3 Hemp Fiber Rope Tensile Test Setup.

3.2.1.2. Concrete Cylinders

To prepare the concrete cylinders, normal strength concrete has been mixed in the structural lab using a medium sized concrete mixing drum. The concrete mix consisted of the following batching weights per cubic meter of concrete: 880 kg of small coarse aggregate, 810 kg of sand, 400 kg of cement and 280 kg of water (water to cement ratio is equal to 0.7). Twelve cylinders of the same batch were cast into moulds, 10 cm in diameter and 20 cm in length, vibrated, then left to cure for 28 days. Another batch of the same mix design was prepared and fifteen cylinders of the same dimensions were cast and were left to cure for 28 days.

3.2.2. Testing Specimens

The purpose of this preliminary study was to evaluate the effect of hemp in confinement as well as to evaluate if surface preparation (such as grinding) would

positively affect the results. Twelve normal weight concrete sample cylinders, 20 cm in length and 10 cm in diameter were prepared as mentioned earlier. After the specimens were allowed to cure for 28 days, four different sets of specimens were prepared: (i) control specimens with no hemp confinement, (ii) epoxy coated specimens with no hemp confinement, (iii) hemp-confined specimens, and (iv) hemp-confined specimens with grinded (roughened) concrete surface. The testing matrix is presented in Table 3.2.

Table 3.2 Concrete Cylinder Test Matrix.

Series #	Series Name	No. of Specimens	No. of Hemp Layers
1	Control (C)	3	-
2	Epoxy (E)	3	-
3	Hemp (H)	3	1
4	Grinded (G)	3	1
	<i>Total number of specimens</i>	12	-

To prepare the hemp-confined specimens, designated as (H), the cylinders were coated with epoxy resin using a brush and then were wrapped manually with hemp fiber ropes in a spiral manner for confinement, fully covering the concrete cylinder with an overlap of 157 mm (half perimeter) at both extremities of the cylinders. The epoxy coated specimens, designated as (E), were only coated with epoxy without any reinforcement. They were prepared to evaluate the epoxy effect without hemp confinement. The grinded specimens, designated as (G), refer to specimens that were roughened prior to wrapping by grinding in order to enhance bonding between the concrete and hemp – epoxy matrix. The wrapping procedure of these specimens was similar to those of (H) series. All test specimens were left to cure for a couple of days

prior to testing. Figure 3.4 shows one control specimen and one hemp-confined specimen prior to testing.



Figure 3.4 Control (Left) and Hemp-Confined (Right) Specimens.

3.2.3. Testing Program

The testing program consisted of axial compression tests conducted on the twelve concrete cylinders, unconfined and confined with hemp fiber ropes previously prepared. The uniaxial compression test was conducted on an Tinius Olsen compression machine under stress control with a constant rate of 0.2 MPa/s based on ASTM C39. Each cylinder was positioned carefully at the center of loading of the machine and four LVDTs were placed 90° apart on 4 sides of the specimen to measure axial strain. Each sample was axially compressed up to failure. Readings from the four LVDTs were averaged and stress strain curves were plotted. The results of the wrapped cylinders were compared with the results of the control cylinders. Test results are presented in the following section. Figure 3.5 shows the testing of one control and one hemp-confined specimen.



Figure 3.5 Test Setup for Compression Test of a Control Specimen (Left), and a Hemp Specimen (Right).

3.2.4. Preliminary Results and Discussion

The stress-strain curves of all the testing series (Control, Epoxy, Hemp, and Grinded) are displayed in Figure 3.6. Each curve is the average of three specimens for each series. It is shown from the stress-strain diagram that these curves can be divided into three regions. The first region of the curves is purely linear in which the stress-strain behavior of the Epoxy, Hemp, and Grinded specimens is similar to the corresponding unconfined Control specimens. The applied axial stress is low in this region; lateral expansion of the confined specimens is inconsiderable and confinement of the hemp fibers is not activated. The second region of the curves is a nonlinear transition region which is reached when the applied axial stress approaches the ultimate strength of the unconfined Control specimens. In this region, considerable micro-cracks are propagated in concrete and the lateral expansion is significantly increased. As the micro-cracks grow, the hemp starts to activate and confines the concrete core to counteract the stiffness degradation of the concrete. The third region is approximately

linear and it represents the fully activated hemp confining the core, which lead to an enhancement of concrete compressive strength and ductility. Failure of the hemp fiber confinement starts when the hoop tensile stress in the fibers exceeds the ultimate tensile strength of the hemp fibers obtained from the tensile test of fibers.

The external confinement provided by the hemp fibers to concrete cylinders gave promising results. Approximately 22% enhancement in the compressive strength was obtained and improvement in ductility was also observed. For the case of hemp-confined cylinders, the enhancement in ductility was 29%, whereas in the case of grinded cylinders, where the concrete surface was roughened to increase the bond between the hemp and the concrete surface, the ductility was enhanced by 35%.

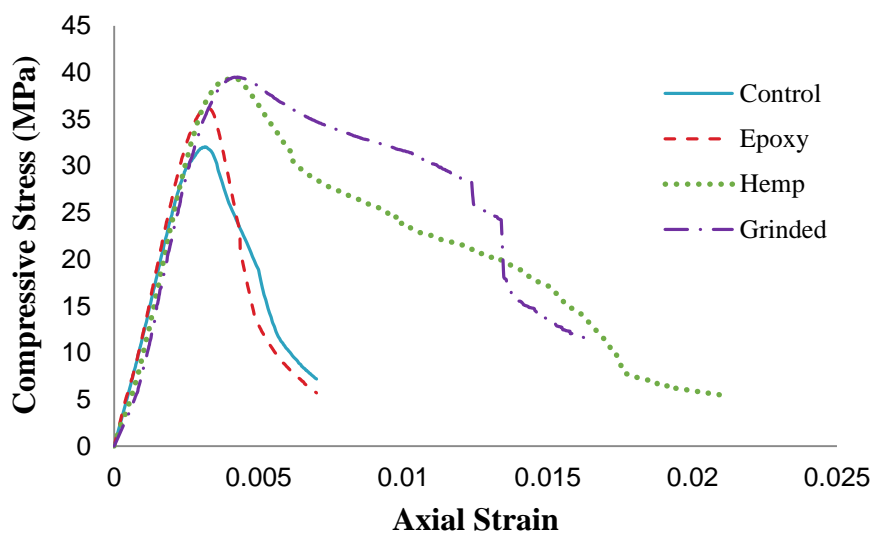


Figure 3.6 Stress-Strain Curves for the Preliminary Study.

3.2.4.1. Failure Mode in Compression

Figure 3.7 shows the failure patterns of the Control and Epoxy specimens. It is observed that the failure of the control specimens is slightly more severe than that of the epoxy painted specimens. The crack widths of the control specimens are clearly larger than those of the epoxy painted specimens; also, some parts of the concrete are crushed and spalled. In Figure 3.8 the failure patterns of hemp-confined cylinders (H-series and G-series) are presented. All confined specimens failed by a sudden rupture in the hemp layer accompanied by a heavy popping noise. The single rupture is not a straight line due to variability of the hemp fibers at different locations. The major crack in the hemp layer was not extended to the top and bottom of the specimens, it was rather concentrated at the middle section of the specimens where the concrete failed and bulged. This implies that the concrete core has already failed before the rupture of the hemp. Therefore, once the concrete core was cracked, the hemp confinement would be activated gradually due to the lateral expansion caused by the gradual crushing and compaction of the concrete. The concrete core has been crushed but remained intact which proves that the confinement effect has been deemed positive to the failure mode of the specimens. Debonding of the hemp layer was observed only in G2 and G3 specimens along the major crack of the specimen.



Figure 3.7 C Type Test Specimens (Left), E Type Test Specimens (Right).



Figure 3.8 H1 Type Test Specimens (Left), G Type Test Specimens (Right).

3.2.5. Summary

This study concerned the axial compressive behavior of hemp fiber confined plain concrete. The experimental results of 12 unconfined and hemp-confined cylinders were presented. The study revealed that hemp fiber confinement enhances the compressive strength and ductility of concrete cylinders. Based on the promising results found in this preliminary study, a bigger scale study was conducted using hemp fiber fabrics as a retrofitting material for masonry.

3.3. Part Two: Strengthening Masonry Walls

This section presents the main part of the study's experimental program. It fulfils the broad objective of the research by strengthening unreinforced masonry walls with externally applied natural hemp fiber fabric and investigating the out-of-plane flexural behavior of the walls. Specimen walls were built and retrofitted with hemp fiber fabric of different configurations, and then the walls were tested against out-of-plane loads. The load-deflection response of masonry walls strengthened with hemp fiber fabric systems when subjected to transverse or out-of-plane loads was determined from static laboratory tests. The performance of the used strengthening technique was determined by examining strength, stiffness, ductility, and failure modes of the wall specimens. The ultimate moment capacity of the unstrengthened walls was estimated using a simple analytical approach and results were compared with the moment capacity calculated according to the Masonry Standard Joint Committee (MSJC 2013) code specifications for masonry structures. A proposed analytical model was used to determine the out-of-plane capacity of the hemp-strengthened walls and results were compared to the experimental results.

3.3.1. Materials

3.3.1.1. Hemp Fibers

In this part of the study, commercial bidirectional hemp fabric was used instead of raw fibers for their ease of use and lower variability. The fabric was supplied in a 1500 mm-wide roll and was cut into designated sizes to conduct this study.

3.3.1.1.1. Tensile Testing of Hemp Fabric

To obtain the tensile strength of the hemp fabric, two samples of hemp fabric were cut into (25 mm x 300 mm) strips. Then the strips were impregnated in epoxy resin and were left to dry after removing any excess epoxy. The strips were allowed to cure for two weeks before testing. The thickness of the strips was measured in three locations along the gauge length (200 mm) of the specimens and averaged due to the variability of the epoxy coating that varied in thickness along each specimen. The average thickness of the strips was 1.2 mm. The tensile testing was done according to the ASTM D 3822-14 the 'Standard for Tensile Properties of Single Fibers' with a constant rate of extension of 1 mm/min for all the tests. This rate of extension was chosen to be the same rate of compression for the wall specimens to keep consistency and represent the real testing conditions that the hemp will be subjected to. Clamps with flat jaws were used to grip the fiber specimens and minimize their slippage. The test setup is shown in Figure 3.9 . The hemp fabric strips were tested in tension up to failure. Fiber extension increases as the load increases until it reaches a peak stress at a certain point of extension and the fabric fiber fails. The load corresponding to the maximum point of extension is the maximum tensile load P_{max} that the fiber can carry. The samples exhibited a sudden brittle failure after reaching the maximum elongation. Results of both samples showed similar load-elongation curves. Figure 3.10 shows the stress-strain diagram of the hemp tensile tests. The average ultimate strain of the hemp fibers, ϵ_{fu} , was 0.0457 and the average tensile modulus was computed to be 1.66 GPa.



Figure 3.9 Tensile Test Setup of Hemp Fabrics

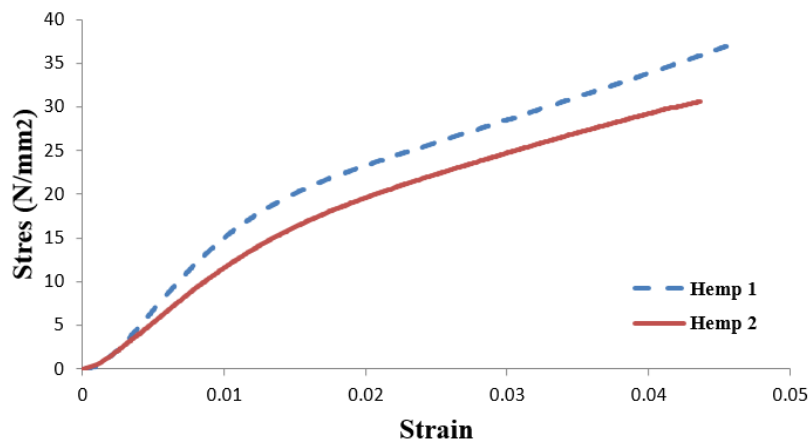


Figure 3.10 Stress-Strain Curve of Hemp Fiber Fabrics.

3.3.1.2. Sikadur 300 Epoxy

Sikadur 300, which is the product of Sika company, was used for strengthening the test specimens. Sikadur 300 is a two-component 100% solids, moisture-tolerant, high strength, and high modulus epoxy and is used as a seal coat and impregnating resin

for horizontal and vertical applications. The mechanical properties of the epoxy are given in Table 3.3 that are taken from the producer specifications.

Table 3.3 Mechanical Properties of Epoxy Resin Sikadur 300.

Tensile Strength (ASTM D-638)	55 MPa
Tensile Modulus (ASTM D-638)	1,724 MPa
Elongation at Break (ASTM D-638)	3 %
Flexural Strength (ASTM D-790)	79 MPa
Flexural Modulus (ASTM D-790)	3,450 MPa

3.3.1.3. Masonry

Normal weight masonry units, 400 mm in length, 200 mm in depth, and 10 mm in thickness, were used for the wall specimens' construction. The masonry units were purchased from a local supplier. Auxiliary tests were performed on individual masonry blocks, mortar cubes, and masonry prisms to determine the mechanical properties of the materials used for the wall construction. To represent the same properties of the walls, all the auxiliary tests were performed on the same day of wall testing. The procedure and results for each test conducted are presented in this section.

3.3.1.3.1. Individual Units

To determine the compressive strength of individual un-grouted hollow concrete masonry units, a total of 6 representative samples of additional masonry units were tested in accordance with ASTM C140/C140M-15. The net cross-sectional area of the units was 21,472 mm².

The ultimate compressive strength of each masonry block was determined using a compression testing machine. Each masonry block was placed in the testing machine where the blocks were subjected to axial load, as shown in Figure 3.11. The axial load was increased until the blocks crushed.

The ultimate load at which the blocks crushed were then recorded, and the ultimate stress, $f'_m(Unit)$, was calculated by dividing the ultimate load by the area of the masonry block. Table 3.4 summarizes the results of the tests. The mean compressive strength for the six masonry units tested was, $f'_m(Unit) = 15.4$ MPa.



Figure 3.11 Individual Concrete Masonry Unit.

Table 3.4 Results of Masonry Unit Compression Test.

Specimen #	Ultimate Load, P (kN)	CMU Area, A (mm ²)	$f'_m(Unit) = P/A$ (MPa)
1	286.2	21,472	13.3
2	333.6	21,472	15.5
3	374.7	21,472	17.4
4	298.7	21,472	13.9
5	291.8	21,472	13.6
6	401.5	21,472	18.7

3.3.1.3.2. Mortar

For the purpose of determining the mortar compressive strength, mortar cube tests were conducted on samples of the mortar used to construct the walls. The mortar cube test according to ASTM C109/C109M required the preparation of 50 mm cube samples of mortar that were tested for their ultimate compressive strength. During the wall construction, the mason was allowed to dictate the quantities of cement, sand, and water in the mortar mix due to his expertise in the field of masonry. Mortar mix water was adjusted two times during the process of constructing the walls in an effort to maintain reasonable workability of the mortar. Three samples of mortar were taken from the mortar batch and placed in 50 mm mortar cube molds made of steel to be tested for compressive strength. The steel cube moulds were greased with petroleum based oil prior to filling with mortar. The mortar samples were moist cured in the molds for 24 hours then released and stored in water for 28 days. The mortar cubes are shown in Figure 3.12.



Figure 3.12 Mortar Cubes.

The ultimate compressive strength for each sample was determined using a compression testing machine. Each mortar cube was placed in the testing machine where the cubes were subjected to axial load. The axial load was increased until the

mortar cubes crushed and the ultimate load was then recorded. The crushed mortar cubes are shown in Figure 3.13. The area of the cube was 2,500 mm². The ultimate stress, f'_{Mortar} , was calculated by dividing the ultimate load by the area of the cube. Table 3.5 summarizes the results from the mortar cube tests. The mean mortar compressive strength from the three tests was, $f'_{Mortar} = 47.3$ MPa.

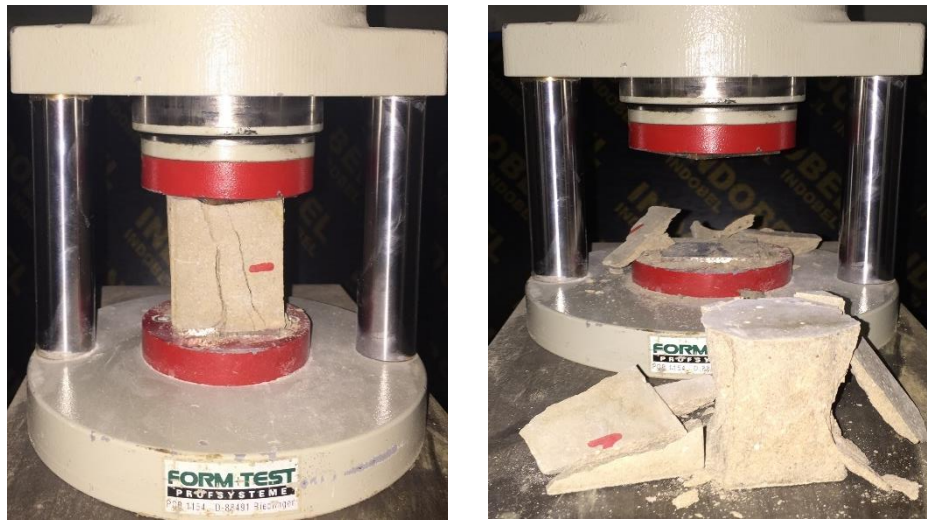


Figure 3.13 Crushed Mortar Cube.

Table 3.5 Results of Mortar Cube Test.

Cube #	Ultimate Load, P (kN)	Cube Area, A (mm ²)	$f'_{Mortar} = P/A$ (MPa)
1	106	2,500	42.4
2	126	2,500	50.4
3	122.7	2,500	49.08

3.3.1.3.3. Prisms

For the purpose of determining the compressive strength of the masonry assemblage, prism tests were conducted on masonry prisms constructed with

representative samples of the concrete masonry units (400 x 100 x 200 mm) and same mortar used to construct the walls. Three masonry prisms were constructed one block wide (400 mm) and three courses high (630 mm). The CMU's were bonded with full mortar beds and mortar joint thickness representative of the corresponding wall specimens (10-13 mm). There was some height variability between the prisms because the masons did not use a leveling line. The average height of the three prisms was 640 mm. The masonry prisms were allowed to cure for 28 days in order to reach ultimate strength. The prisms were tested according to ASTM C1314-14.

The ultimate compressive strength for each masonry prism assemblage was determined using the MTS testing machine. Each prism was placed in MTS where the masonry prisms were subjected to axial load, as shown in Figure 3.14. The axial load was increased until the prisms crushed and the ultimate load was then recorded. The net cross-sectional area of the prism was taken as the net cross-sectional area of masonry units, which was computed to be 21,472 mm². The ultimate stress, $f'_m (Prism)$, was calculated by dividing the ultimate load by the area of the prism. Table 3.6 summarizes the results from the prism tests. The mean compressive strength from the three prism tests was, $f'_m (Prism) = 11.2$ MPa.

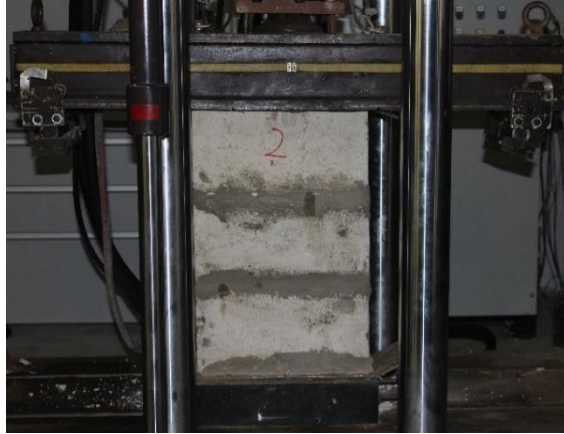


Figure 3.14 Masonry Prism.

Table 3.6 Results of Prism Test.

Prism #	Ultimate Load, P (kN)	Net Area, A (mm²)	$f'_m (Prism) = P/A$ (MPa)
1	215.09	21,472	10.0
2	210.64	21,472	9.8
3	296.16	21,472	13.8

3.3.2. Test Specimens

3.3.2.1. Wall Details

The wall test specimens were constructed in five series of different hemp fiber reinforcement configuration. Each series consisted of two wall specimens. A total of ten wall specimens, 2,050 mm in length, 630 mm in width, and 10 mm in thickness, were prepared using 400 x 100 x 200 mm normal weight hollow concrete masonry units. Each wall specimen was 3 courses high without any type of reinforcement.

The wall dimensions were selected based on available resources in the laboratory. Also, since many facilities were constructed using a running bond, the walls were constructed in running bond and the joints were finished flush with the outside of

the masonry units. All specimens were allowed to cure for at least 28 days before the hemp fiber fabric reinforcement was applied.

3.3.2.2.Reinforcement Strategy

Series one involved two unreinforced wall specimens as control specimens. Each of series two, three, four, and five consisted of two strengthened wall specimens. These wall specimens were strengthened with hemp fiber fabric applied to the surface of the wall by using epoxy as the bonding agent. Each series had a different reinforcement scheme. The different hemp fabric reinforcement configurations investigated were: (i) horizontal and vertical strips covering only 50% of the tension side of the wall with anchors, (ii) fully covered from the tension side of the wall with one layer without anchors, (iii) fully covered from the tension side of the wall with one layer with anchors, and (iv) fully covered from the tension side of the wall with two layers with anchors. Table 3.7 and Table 3.8 summarize the testing matrix and its details, respectively. Figure 3.16 shows the different layout patterns of the hemp reinforcement. Anchors made up of additional hemp fiber fabric were installed and wrapped around in a U-shape to the back of the walls. Although this kind of anchorage system is not very practical for the real structure, it has been chosen so for this experimentation to avoid premature de-bonding failure of the hemp fiber fabric at the ends of the wall test specimens during testing prior to attaining full strength capacity.

Table 3.7 Masonry Walls Testing Matrix.

Series #	Series Name	No. of Specimens	No. of Layers	Strengthening Scheme	Anchors
1	Control	2	--	--	--
2	H S	2	1	Horizontal & Vertical Strips (one side)	Yes
3	H 1	2	1	One side fully covered	No
4	H 2	2	1	One side fully covered	Yes
5	H 3	2	2	One side fully covered	Yes



Figure 3.15 Strengthened Test Wall Specimens.

Table 3.8 Test Matrix Details.

Series Name	Wall Identifier	Fiber Orientation	No. of Layers	No. of Strips	Reinforcement Ratio (%)	Surface Area Ratio (%)
Control	C1	--	--	--	--	--
	C2	--	--	--	--	--
H S	HS-a	0°	1	2	0.381	51.3
		90°	1	4	--	--
	HS-b	0°	1	2	0.381	51.3
		90°	1	4	--	--
H 1	H1-a	0°	1	1	1.2	100.0
	H1-b	0°	1	1	1.2	100.0
H 2	H2-a	0°	1	1	1.2	100.0
	H2-b	0°	1	1	1.2	100.0
H 3	H3-a	0°	2	1	2	100.0
	H3-b	0°	2	1	2	100.0

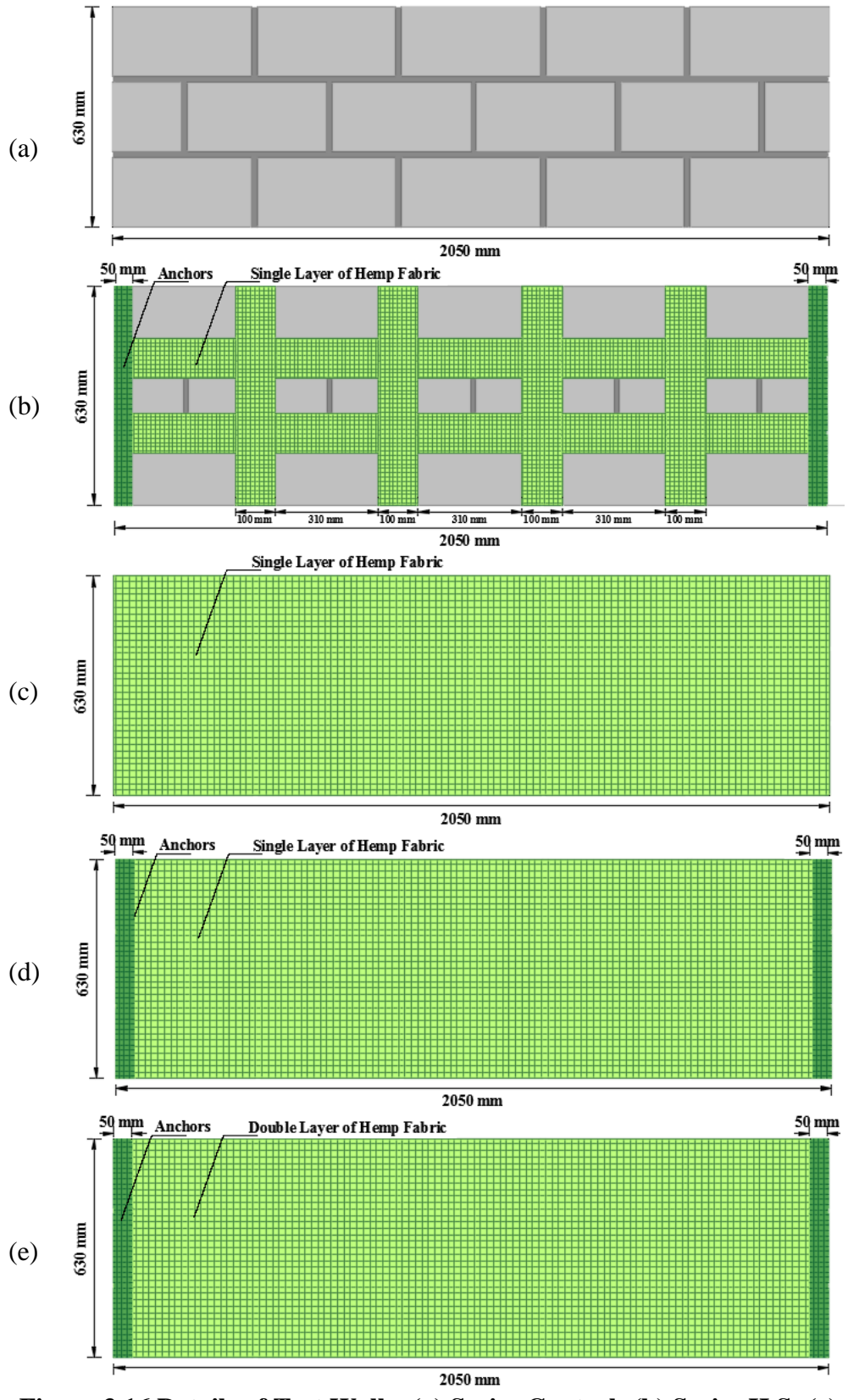


Figure 3.16 Details of Test Walls: (a) Series Control; (b) Series H S; (c) Series H 1; (d) Series H 2; (e) Series H 3.

3.3.2.3. Wall Construction

In this section, a detailed procedure of the construction of the masonry wall test specimens is described. It is noted that all ten wall test specimens were constructed during the same day with the same materials and labor. The mason constructed all wall specimens using typical masonry construction techniques practiced in the masonry industry.

The floor of the structural lab where the walls were constructed was first covered with a thin layer of plastic sheet for the ease of handling and movement of the wall specimens to the testing machine. In order to secure the first course of CMU, a layer of mortar was used to bond the CMU's to the floor. The first course of CMU consisted of 5 masonry units laid horizontally as shown in Figure 3.17 (left). Once the first course was secured, the remaining 3 courses were laid. The mortar was applied on top of the first course. With the use of a mason's trowel, the mortar was applied evenly over the entire top side of the CMU's. The next course of CMU's was then placed atop the mortar joint, as shown in Figure 3.17 (right).



Figure 3.17 Mason Laying First and Second Course of CMU.

The mason placed each CMU carefully on top of the mortar joint and positioned them into place by tapping the top and sides of the unit with the mason trowel. Mortar was added to the ends of the CMU's prior to positioning them on the mortar joint to create vertical head joints. The mortar joints between the CMU courses were in the range of 10 mm to 13 mm. With the use of a level, the mason leveled all CMU's in and out of plane of the wall.



Figure 3.18 Mason Leveling the Walls.

The mason continued the process of laying the mortar and CMU's until each wall reached its full height and full length. Then the mason filled any unfilled or partially filled joints in the wall with mortar to fully bond the CMU's together. The final dimensions of the masonry walls were 2050 mm in length and 630 mm in width. After all the walls were constructed and ready, they were allowed to cure in a moist environment for 28 days before any application of reinforcement.



Figure 3.19 Fully Constructed Masonry Walls.

3.3.3. Hemp Fiber Fabric Installation

3.3.3.1. Surface Preparation

The surface of the masonry walls was prepared before the hemp fiber fabric could be applied to the walls. In order for the hemp fiber fabric to completely adhere to the masonry, the surface of the walls should be smoothed out and cleaned from any dust and impurities. First, the surface of the walls was abraded using an electric orbital sander to smooth out all irregularities of the masonry. Then, using a coarse wire brush, the surface of the walls was cleaned from dust and impurities.



Figure 3.20 Surface Preparation for Hemp Fiber Fabric Installation.

3.3.3.2. Cutting Fabric

Since the hemp fiber fabric came in a 1500 mm wide roll, the material was cut into the required width and length prior to installation, as seen in Figure 3.21. The 1500 mm wide roll was placed on a clean floor and with the use of a metal ruler and scissors, the fabric was carefully measured and cut in length and width into the desired fabric size. Eight sheets of fabric were measured and cut into 2100 mm in length and 650 mm in width, to fully wrap 4 walls with one layer and 2 walls with 2 layers of fabric on one side of the masonry walls. For the (HS) wall series, horizontal fiber strips, 2100 mm in length and 100 mm in width, and vertical fiber strips, 650 mm in length and 100 mm in width, were measured and cut. Each of the walls will be reinforced with two horizontal strips and four vertical strips.

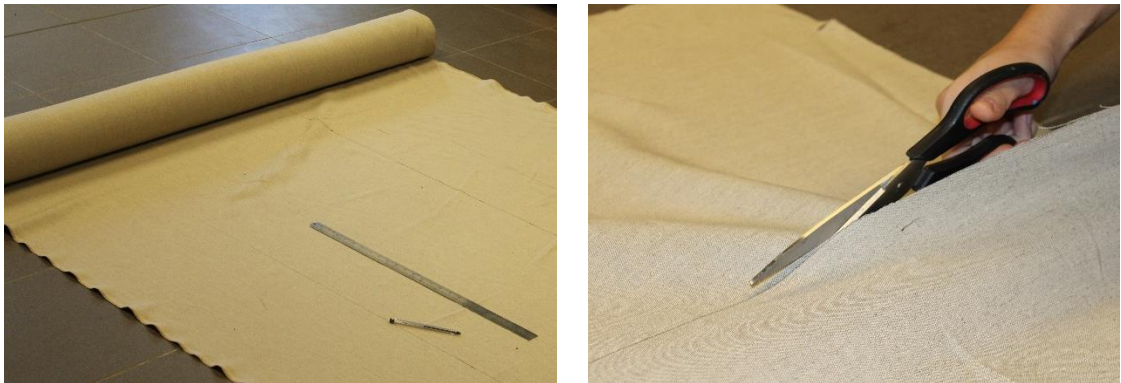


Figure 3.21 Cutting Hemp Fiber Fabric into Desired Width and Length.

The fabric was intentionally cut longer by 50 mm and wider by 20 mm in order to wrap the edges at the ends. Additional fabric was needed to form anchors at the two horizontal ends of the walls to avoid failing by debonding. The anchors were measured and cut to be 600 mm long and 650 mm wide.

3.3.3.3. Primer Surface

In order to prevent the masonry surface from drawing epoxy resin from the hemp fabric as well as to promote adhesion, a layer of epoxy resin should be applied. A batch of epoxy was mixed as proposed by the producer company user manual and placed in a rectangular flat container; then, a layer of epoxy primer was applied to the surface of the masonry walls using a roller until the masonry surface was locally saturated, as seen in Figure 3.22. The primer used was the Silkadur-300, the same epoxy used to apply the hemp fiber fabric onto the walls. The primer was applied on the side of the walls where the fabric was to be placed. Also, primer was applied on the edges of the walls where the anchors were to be placed. The walls were left to cure for 48 hours before the application of the fabric on the surface.



Figure 3.22 Application of Primer prior to Hemp Fiber Fabric Installation.

3.3.3.4. Installation of Hemp Fabric Reinforcement

After the walls cured for 48 hours, the hemp fabric reinforcement was installed on the surface of the walls in several steps. First, the walls were laid horizontally and a

layer of Silkadur -300 epoxy was applied to the surface. Next, for the fully wrapped walls, the fabric was placed onto the wall surface and was saturated with epoxy resin using a roller. After all the fabric was saturated, it was smoothed out using the hands to make sure no air bubbles were trapped between the fabric, epoxy resin, and the masonry wall surface. Finally, a final layer of epoxy was applied onto the fabric. All the hemp fiber fabric reinforcement was installed during the same day for all the wall specimens. After all the walls were reinforced, they were left to cure for 48 hours.



Figure 3.23 Installation of Hemp Fabric to Masonry Wall (Series H1, H2, and H3).

For the walls wrapped with 100 mm fiber strips, a layer of epoxy was applied on the walls prior to installing the fabric strips. Then the fabric was saturated with epoxy resin using a brush and placed onto the wall surface. The horizontal strips were installed on top of the horizontal mortar joints first, smoothed out to remove all air bubbles, and covered with another layer of epoxy. The same procedure was applied to the vertical strips, which were installed on top of the vertical mortar joints. After installing each fiber strip, it was smoothed out using the hands to make sure no air bubbles were trapped between the fabric, epoxy resin, and the masonry wall surface. Finally, a final layer of epoxy was applied onto the fabric.

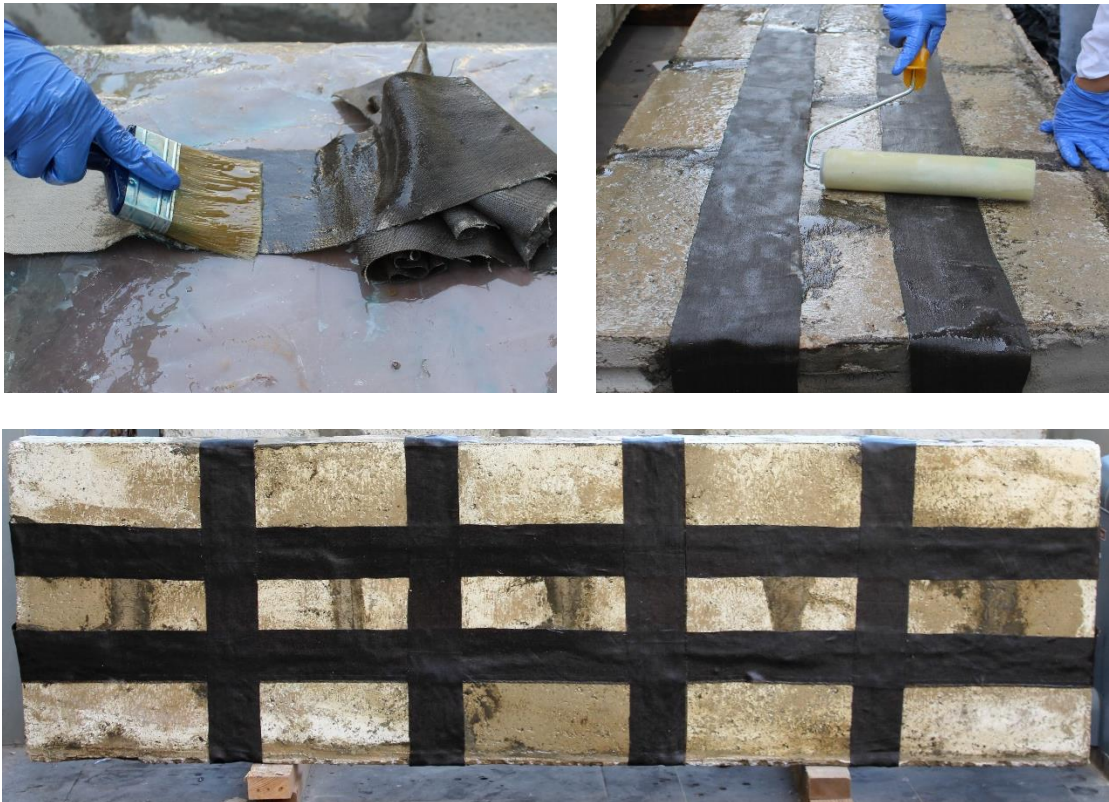


Figure 3.24 Application of Hemp Fabric to Masonry Wall (Series HS).

3.3.3.5. Anchoring

As mentioned earlier, the purpose of installing additional fabric at the ends of the walls is to act as an anchorage system to prevent premature de-bonding of the hemp fiber fabric during testing. According to the test matrix presented earlier, all strengthened walls except for walls H1-a and H1-b of series H 1 will have anchors installed at their ends. The reason for this is to study the effect and compare the behavior of the anchored and the non-anchored walls.

Once the walls cured for 48 hours, the anchors were installed onto the walls of series H 2, H 3, and H S. First, the anchors were soaked in the same epoxy resin used to install the hemp fiber fabric reinforcement, then were applied at the ends of the walls and wrapped around in a U-shape to the back of the walls, as shown in Figure 3.25. The anchors were allowed to cure for at least 48 hours before initiating testing of the walls.



Figure 3.25 Application of Anchors at the End of a Masonry Wall.

3.3.4. Analytical Modelling

In this study, the section analysis procedure was followed in order to calculate the out-of-plane capacity of both unstrengthened and hemp fiber fabric-strengthened URM walls. Load carrying capacity calculations for strengthened masonry walls with hemp fiber fabric are presented based on strain compatibility and force equilibrium. The following subsections present the details of the procedure.

3.3.4.1. Unstrengthened Walls

3.3.4.1.1. Proposed Methodology

The ultimate moment capacity of an unstrengthened control specimen is assumed equal to its cracking moment, which depends on the masonry's modulus of rupture f'_r . In this study, the modulus of rupture of concrete masonry elements is assumed to be 0.10 of the minimum compressive strength, f'_m , obtained for mortar cubes, individual masonry units, and masonry prisms as follows

$$f'_{Mt} = 0.1 \times \min(f'_{m(mortar)}, f'_{m(units)}, f'_{m(prisms)}) \quad (1)$$

The flexural failure load of the unstrengthened control walls specimens, M_u , was determined such that it induces the first crack in the tension (bottom) side of the wall specimen. The cracking moment is computed from

$$M_u = M_{cr} = \frac{f'_r I}{y_t} = \frac{f'_r w t_m^2}{6} \quad (2)$$

where w = total width of the masonry wall; and t_m thickness of masonry wall.

3.3.4.1.2. Building Code Requirements for Masonry Structures

The cracking moment capacity of the unstrengthened walls was also computed using the Masonry Standards Joint Committee (MSJC 2013). This code covers the design and construction of masonry structures. According to Section 9.1.9.2 of the MSJC code (MSJC 2013), the modulus of rupture, f_r , for masonry elements subjected to out-of-plane or in-plane bending shall be in accordance with the values in Table 9.1.9.2. The moment capacity was calculated using Equation (1) with the modulus of rupture obtained from Table 9.1.9.2 of the MSJC code.

3.3.4.2. Hemp-Strengthened Walls

3.3.4.2.1. Proposed Methodology

In this section, the derivation for the nominal moment capacity for masonry walls reinforced with hemp fiber fabric is presented. The derivation is a simplified analytical method based on force equilibrium and strain compatibility with the following assumptions:

- Sections perpendicular to the axis of bending that are plane before bending remain plane after bending and strain in masonry and hemp fiber fabric shall be directly proportional to the distance from the neutral axis;
- The tensile strength of masonry is ignored and does not contribute to the flexural strength of the walls; and
- There is a perfect bond between the hemp composite and the masonry and thus there is no relative slip between the two;

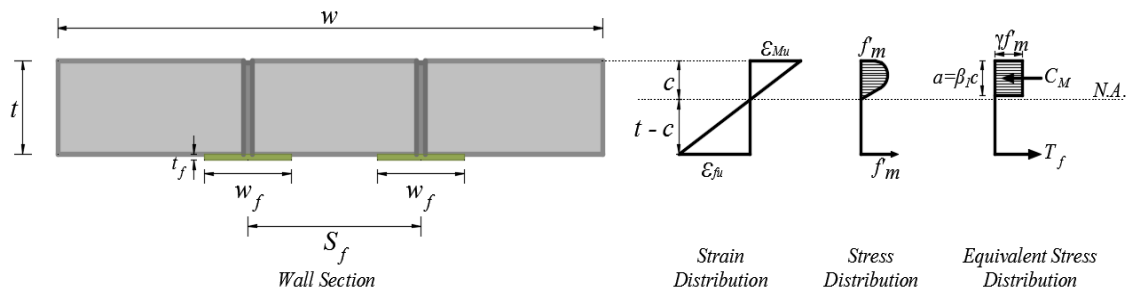


Figure 3.26 Internal Strain and Stress Distribution for a Typical URM Wall Section Strengthened with Hemp Fiber Fabric.

Figure 3.26 shows a free body diagram of the cross section of the hemp-strengthened masonry wall with the variation of strain and stress under out-of-plane loading. A linear strain distribution was assumed for the section. For the evaluation of the nominal moment capacity of the section, the strain in the extreme compression fiber is set equal to the maximum useable strain, ϵ_{mu} . In this study, the maximum useable strain in the masonry at the extreme masonry compression fiber was taken to be 0.0025 per Section 9.3.2 of the MSJC code (MSJC 2013). Above the neutral axis, the masonry compression stress distribution was simplified and modeled as a rectangular uniform stress block with the maximum compression stress taken to be 80% of f'_M (MSJC, 2013). The stress block was taken to be located at a distance $a = 0.8 c$ from the fiber of maximum compressive strain (MSJC 2013). From the stress diagram in Figure 3.26, the compressive force resisted by masonry, C_M , and the tensile force of the hemp composite, T_f , were computed from:

$$C_M = 0.8 f'_M a w = 0.8 f'_M w 0.8 c \quad (3)$$

$$T_f = A_f f'_{fu} = A_f \epsilon_f E_f$$

where, w is the width of the wall; f'_M is the ultimate strength of masonry; f'_{fu} is the ultimate strength of the hemp composite; ε_f is the hemp fiber fabric strain; E_f is the Young's Modulus of the hemp fiber fabric; and A_f is the total cross-sectional area of externally bonded hemp composites given by

$$A_f = n_s \times n_l \times w_f \times t_f \quad (4)$$

where, n_s is the number of hemp fabric strips applied to the wall; n_l is the number of hemp fabric layers; w_f is the width of hemp fabric strip; and t_f is the thickness per layer of hemp fabric composite. The location of the neutral axis was computed from the equilibrium of internal forces as follows

$$C_M = T_f$$

$$0.8 f'_M w 0.8 c = A_f \varepsilon_{fu} E_f \quad (5)$$

$$0.8 f'_M w 0.8 c - A_f \varepsilon_{fu} E_f = 0$$

The ultimate flexural strength can then be determined from

$$M_n = T_f \left(t - \frac{a}{2} \right) \quad (6)$$

$$M_n = A_f \varepsilon_{fu} E_f \left(t - \frac{0.8 c}{2} \right)$$

or in terms of masonry compressive strength

$$M_n = C_M \left(t - \frac{a}{2} \right) \quad (7)$$

$$M_n = 0.8 f'_M 0.8 c w \left(t - \frac{0.8 c}{2} \right)$$

3.3.5. Testing Program

3.3.5.1. Test Setup

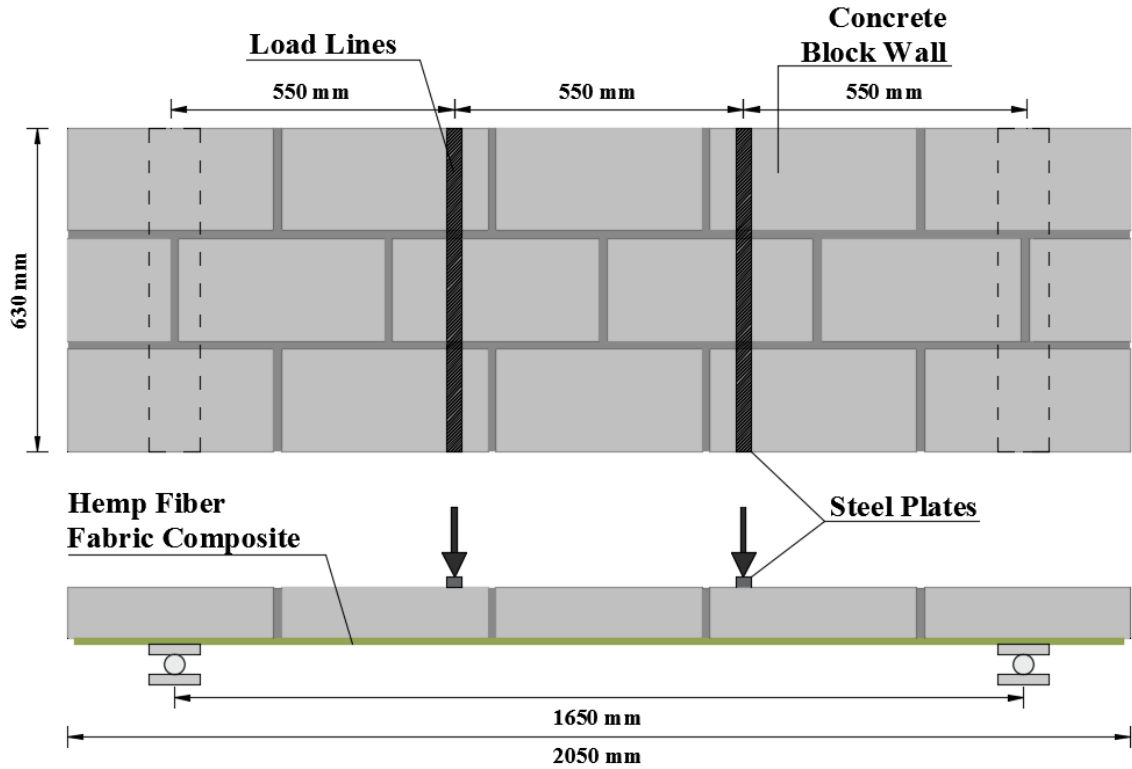


Figure 3.27 Test Setup and Dimensions of the Wall Specimens.

All wall specimens were tested monolithically to failure under simply supported conditions in the test setup shown in Figure 3.27. The walls were tested with third-point loading as a simply supported beam to model out of plane horizontal forces. The walls were placed in a horizontal position with span direction parallel to the mortar bed joints. The test specimen was supported by a steel rod, 15 mm in diameter and 600 mm in length, placed between two steel plates on each side of the wall at a distance of 200 mm from the wall edge. The steel plates had a groove at their mid-span along their length in order to allow the steel rods to roll in place. The bottom plate was fixed onto a steel frame while the top plate was free to rotate. This support system, shown in

Figure 3.28, acted as roller supports restraining only the vertical movement during loading and allowing for rotation and horizontal movement.

Loading was applied to the test specimens by a hydraulic piston that supplied the load which was transferred to the wall using a distribution frame. The load was centered on the distribution frame which then separated the concentrated load into two line loads located $\ell_{span}/3$, or 550 mm, center-to-center apart and $\ell_{span}/3$, or 550 mm, center-to-center from each support. The line loads loaded two steel plates, 50 mm wide and 5 mm thick, that rested along the full width of the walls. The applied loading was measured electronically with a load cell capacity of 100 kN in compression.



Figure 3.28 Wall Support.

3.3.5.2. Instrumentation

The instrumentation of the test setup consisted of various Linear Variable Differential Transducers (LVDT's) to measure deflections. Two support and midpoint deflections of the test specimens were measured using a total of six LVDTs. Since the

loading frame prevented measuring of the mid-span, two LVDTs were placed on both sides of the frame along the centerline of the specimen. The deflection readings will be then averaged to obtain one deflection value for the midspan. For consistency, to measure deflection near the supports, two LVDTs were placed at $\ell_{span}/6$ away from each support along the same line on both sides of the wall. The deflection readings will be averaged to obtain one deflection value along the centerline of the specimen near both supports. The LVDTs were placed on the top side of the wall specimens. By positioning the LVDTs on the top side, all deflection values that the LVDTs measured were in the negative sign. The location of the LVDTs was the same for all wall specimens for consistency. Figure 3.29 shows positions of LVDTs along the wall span.

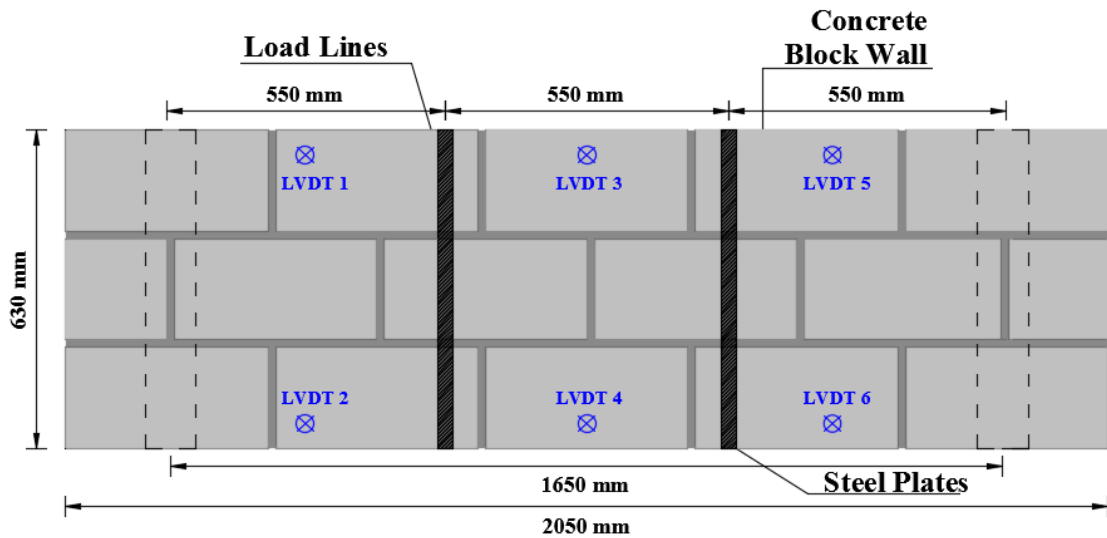


Figure 3.29 Instrumentation Layout.

3.3.5.3. Test Procedure

Each wall specimen was transported to the MTS using a manual forklift. Metal chains were then wrapped around each wall and with the aid of an overhead crane, each wall was lifted and positioned onto the MTS as shown in Figure 3.30. While the wall

was still lifted, the steel supports were inserted underneath the wall, 200 mm away from its edges. Then the wall was carefully lowered until it rested on both supports in their designated position and was centered on the MTS. Then the LVDTs were positioned on the on top of the wall in the locations shown in Figure 3.29. The experimental wall setup is presented in Figure 3.31. After the specimen was properly aligned, load was applied at a rate of 1 mm per minute. The test was controlled using an existing computer controlled data acquisition system and all electronic readings were recorded using this system.



Figure 3.30 Positioning Wall Specimen into MTS Machine.

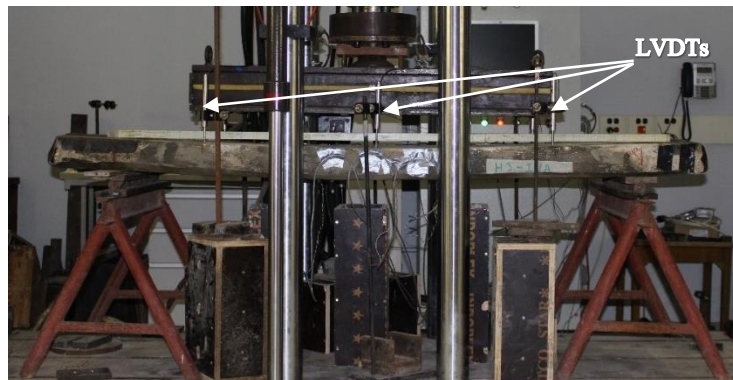


Figure 3.31 Test Setup of the Walls.

CHAPTER 4

DISCUSSION OF TEST RESULTS AND ANALYSIS

4.1. Introduction

In this chapter, the experimental results obtained from the masonry walls testing program will be presented and analyzed. During the test, the behavior of each wall specimen was monitored, including its deflection and failure mode. Therefore, for each specimen its load-deflection curve and the mode of failure will be presented. The analytical model presented earlier will be validated against the experimental results as well.

4.2. Load – Deflection Behavior

The load-deflection curve of the control wall (C1) is illustrated in Figure 4.1. The response is generally linear until one of the mortar joints loses its ability to carry the load and separates and the wall fails in a brittle manner. The second control wall (C2) was not tested because it failed while transporting the wall onto the MTS due to mishandling. Figures 4.2 to 4.8 show the individual load-deflection response of series HS, H1, H2, and H3 walls, respectively. The graphs present load registered versus measured left, right, and midspan deflection. The response of the wall HS-a has been disregarded due to testing malfunction and only wall HS-b will represent the series HS. The overall response of the strengthened walls can be divided into two phases. The first phase of the response is almost linear which continues until around 0.7 – 1.2 mm of midspan deflection. During this phase, the mortar between the joints reaches its tensile

capacity which leads to the initiation of cracking. As the bond between mortar and one block is lost, a joint separates and the load is transferred to the next joint. This is continued until the joints in the maximum moment region of the wall are completely separated.

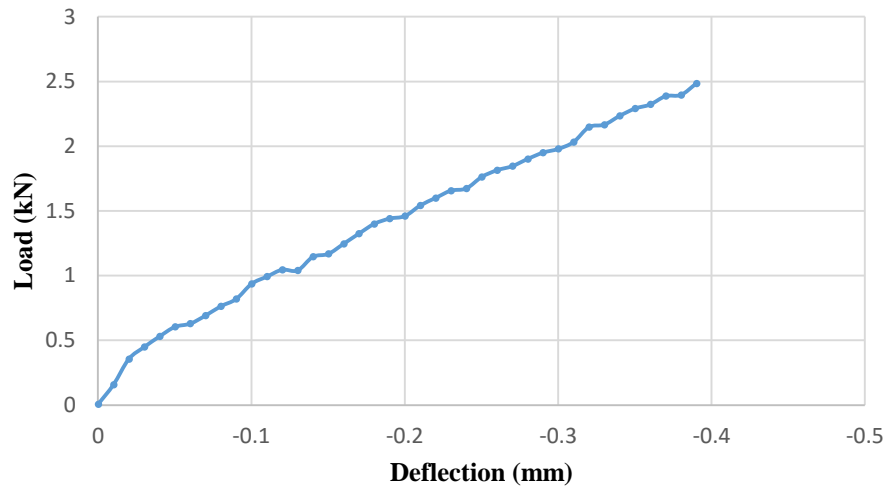


Figure 4.1 Load-Midspan Deflection Response for Control Wall C1.

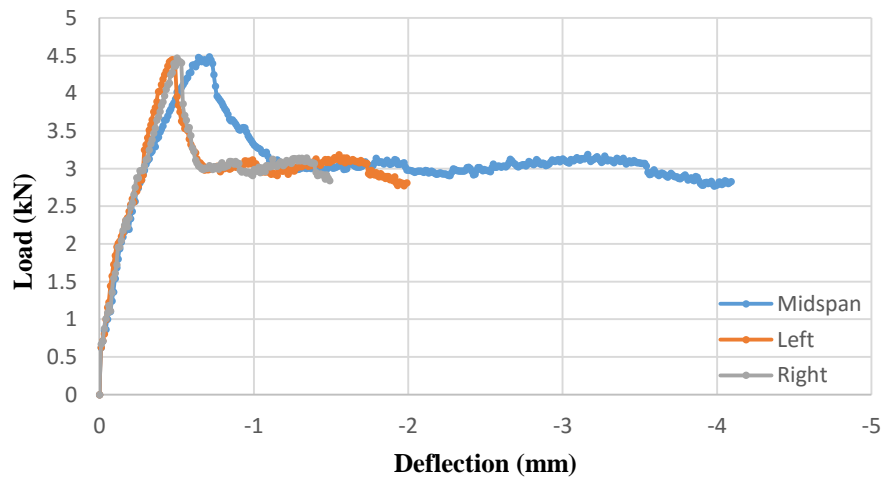


Figure 4.2 Wall H S-b Load-Deflection Response.

The second phase of the response is a non-linear stage where large deflections begin to be registered for small increments of loads. It is identified by a reduction in the flexural stiffness of the specimen due to joint separation. At this stage, the mortar no longer contributes to the tensile capacity of the wall and has no effect on the load-deflection behavior of the wall. The flexural stiffness of the wall is now a function of the Hemp fiber reinforcement ratio and this portion of the load-deflection curve signifies the role of the Hemp fiber reinforcement to the performance of the specimen. The hemp reinforcement is fully activated. For the rest of the test, micro cracks develop in the masonry blocks and the crack widths in the mortar joints gradually increase as the wall experiences more deflection with the incremental increase in load. A change in the color of the hemp fibers is also noticed, indicating the stretching that the material is undergoing.

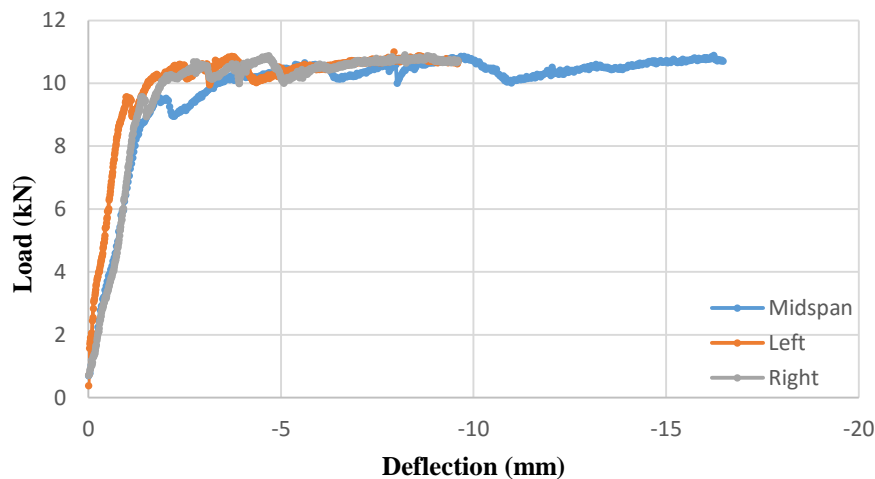


Figure 4.3 Wall H 1-a Load-Deflection Response.

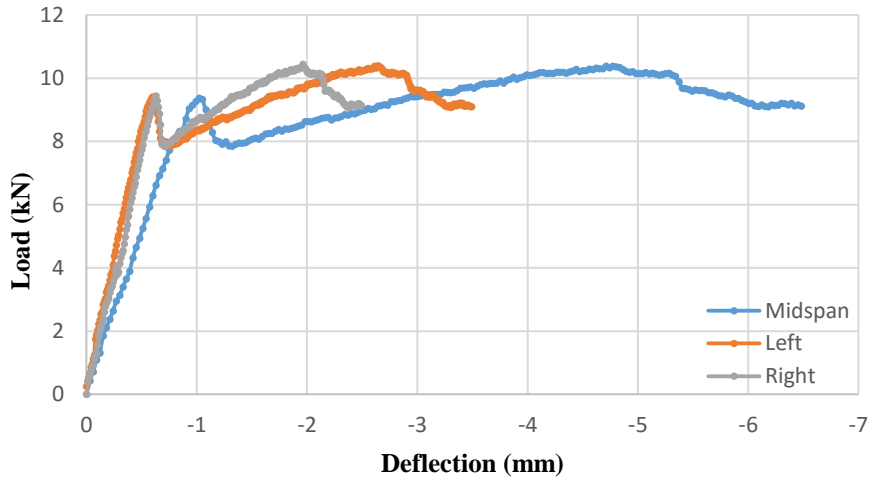


Figure 4.4 Wall H 1-b Load-Deflection Response.

It can be seen from the load-deflection curves the occurrence of drastic drops as well as minor drops in the registered loads. The drastic drops indicate the development of new cracks in the wall, whereas the minor drops in loads indicate that the existing cracks were widening or spreading in depth. It is also noticed from the load-deflection curves that after each drop, the load recovers to a higher level but with a reduced stiffness.

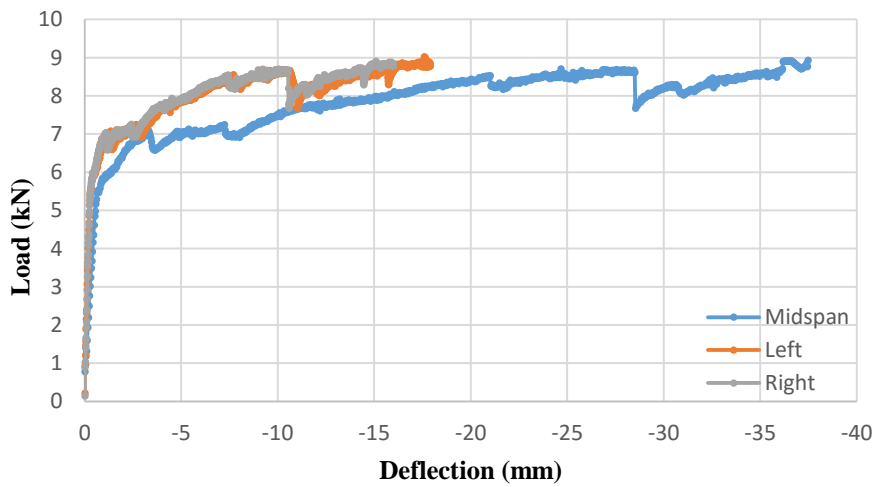


Figure 4.5 Wall H 2-a Load-Deflection Response.

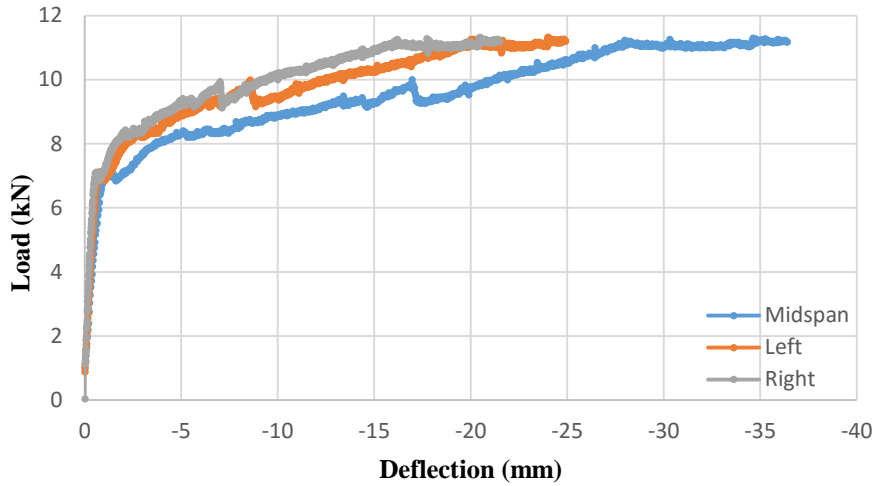


Figure 4.6 Wall H 2-b Load-Deflection Response.

The poor performance of the control wall C1 in strength and deflection represents the significant effect that the application of the least quantity of hemp fiber fabric reinforcement can have on the flexural performance of the masonry walls. More notably, the brittle failure is substituted with sufficient deflection of the walls after the first crack.

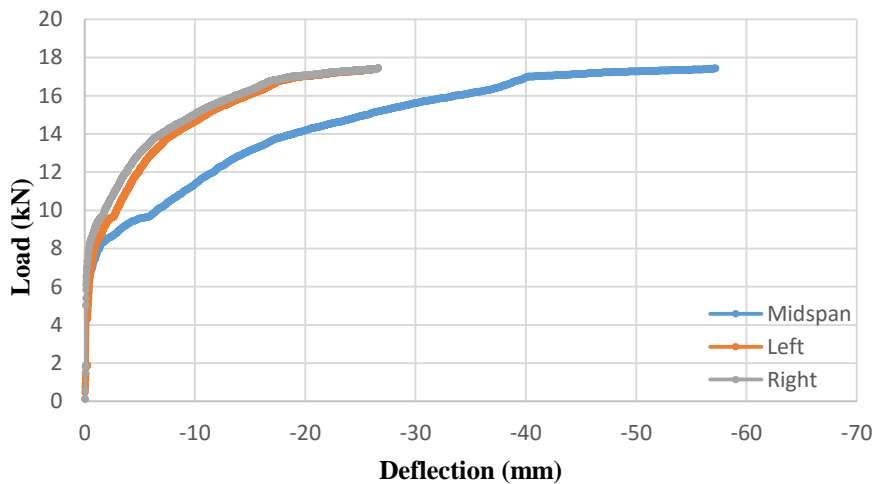


Figure 4.7 Wall H 3-a Load-Deflection Response.

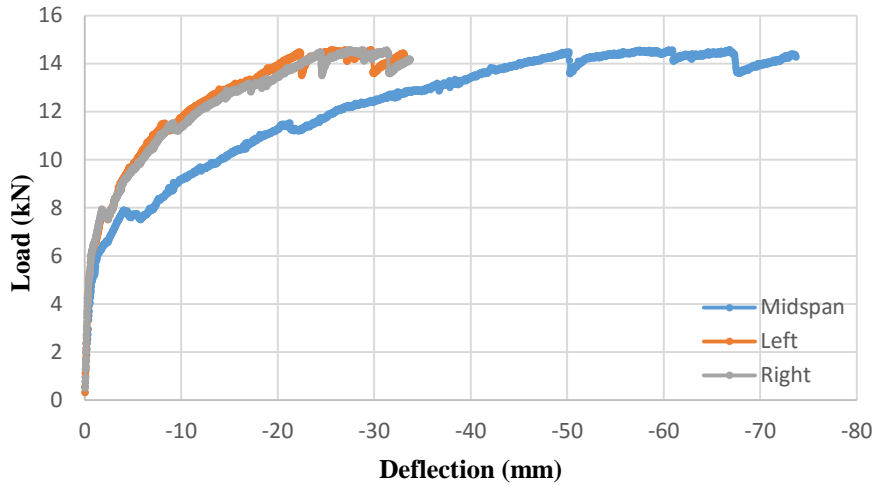


Figure 4.8 Wall H 3-b Load-Deflection Response.

It is important to note that masonry in general is a very variable material. Thus, the two phases of response of the load-deflection curves were evaluated to show ranges of performance or behavior. These evaluations should not be taken in terms of exact values. To minimize the variability of the results, the load-deflection curves of each series were averaged and the combined curves of all the series are shown in Figure 4.9.

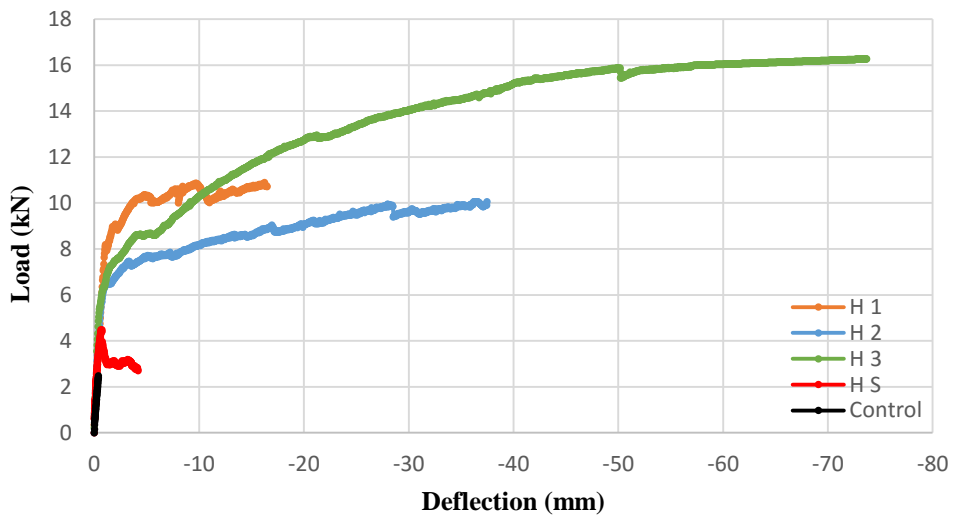


Figure 4.9 Comparison of Load-Midspan Deflection Response of All Series.

The wall deflection along the length was plotted for one specimen of each series at loads 2, 4, 6 and 10 kN shown in Figure 4.10 to Figure 4.13. Also, the ultimate deflection of the wall along the length was plotted for one specimen of each series at their ultimate loads shown in Figure 4.14. The plots show how the deflection of the walls increased significantly with increase in the reinforcement ratios of the wall in contrast to the very small deflection of the unstrengthened control wall. The ultimate midspan deflection of the unstrengthened wall was only 0.4015 mm, while the ultimate midspan deflections of the strengthened walls were 4.162, 16.47, 37.47, and 73.68 mm for series HS, H1, H2, and H3, respectively.

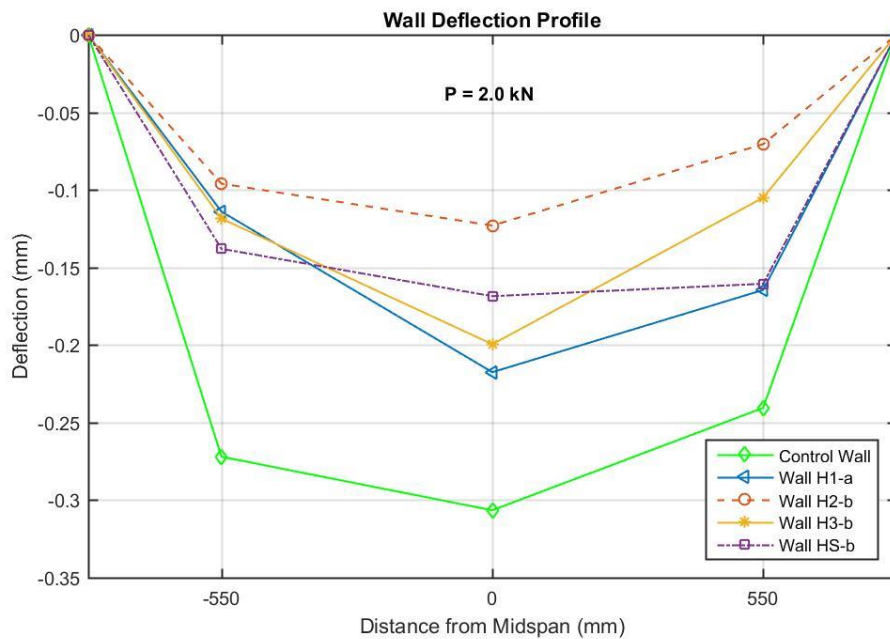


Figure 4.10 Wall Deflections along the Length at P= 2 kN.

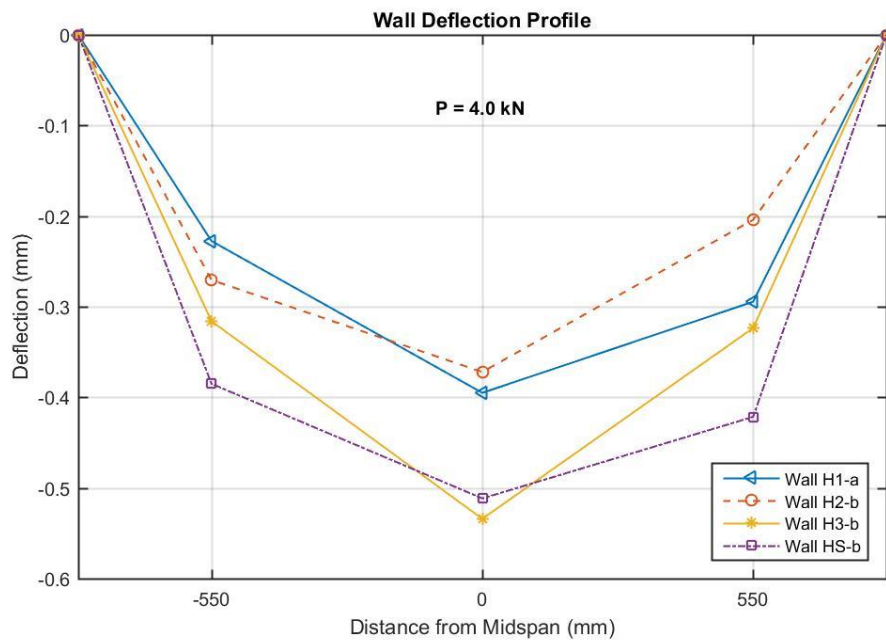


Figure 4.11 Wall Deflections along the Length at P= 4 kN.

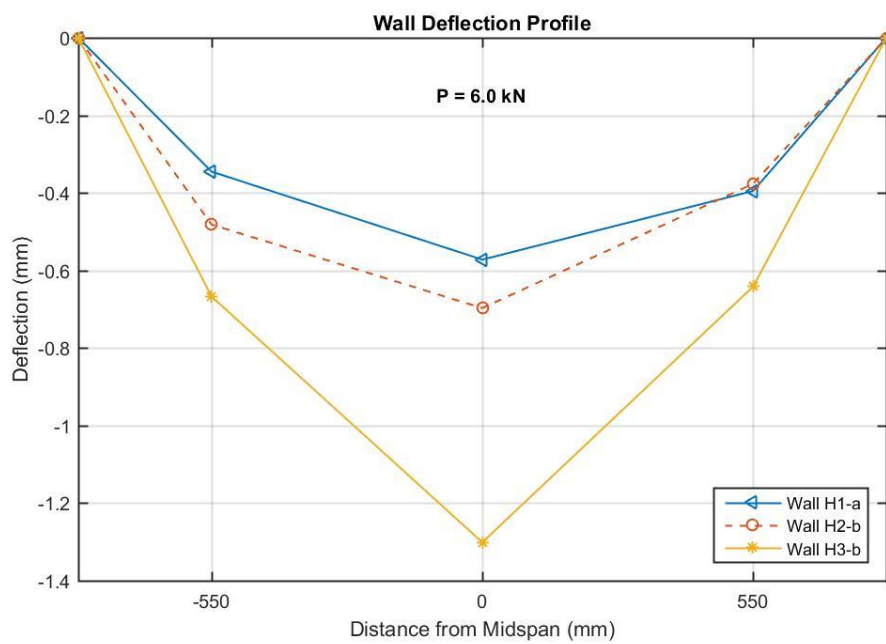


Figure 4.12 Wall Deflections along the Length at P= 6 kN.

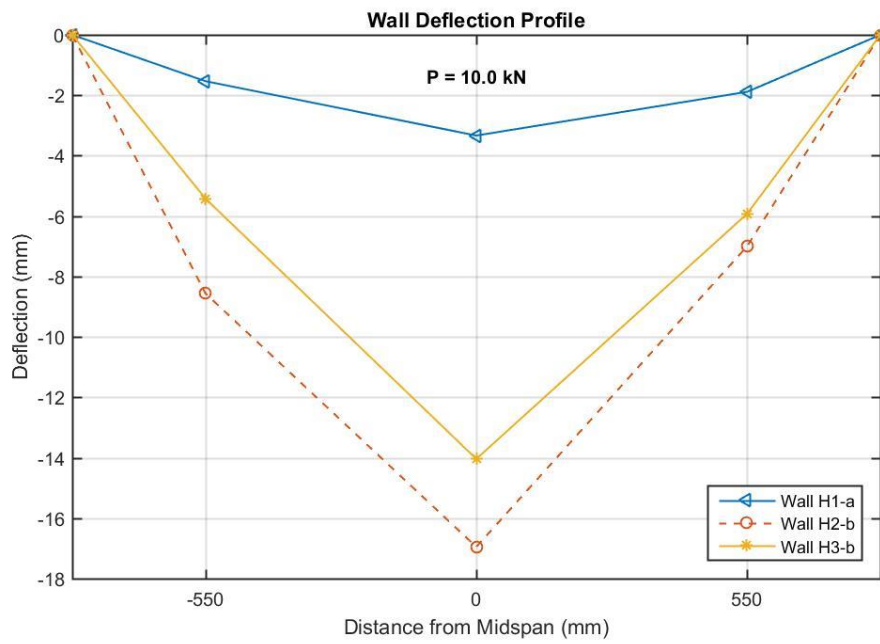


Figure 4.13 Wall Deflections along the Length at P= 10 kN.

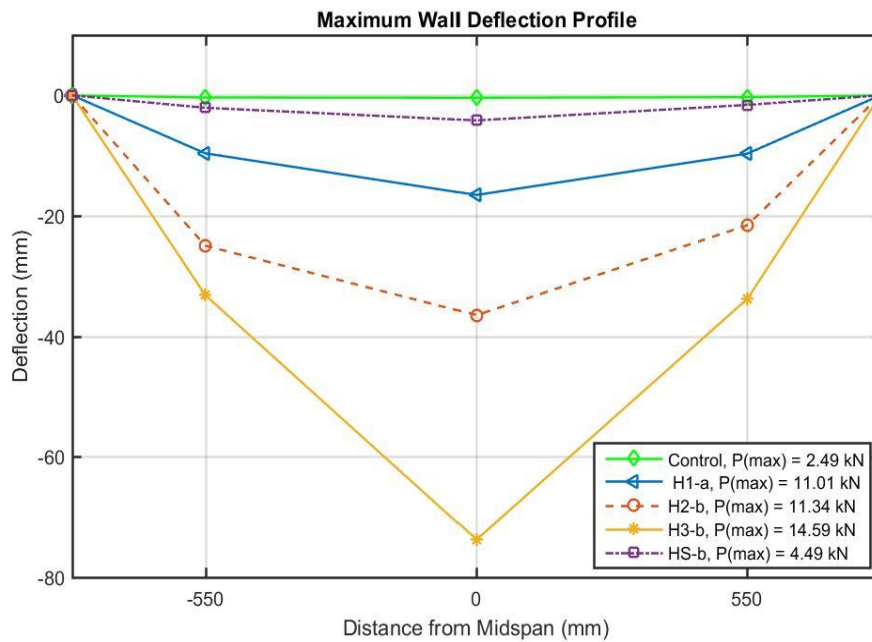


Figure 4.14 Maximum Wall Deflection at Ultimate Loads.

4.3. Performance of Strengthened Walls

4.3.1. Flexural Strength Capacity

It is observed from the load-deflection responses that the out of plane strengths of masonry walls are increased significantly with the applied strengthening method. The unstrengthened control wall specimen failed under a very low out of plane force with slight deflection. Figure 4.15 illustrates the effect of hemp reinforcement ratio ρ_f on the performance of the test walls in terms of percent gain in out-of-plane capacity with respect to the control specimen. As series H1 and H2 have the same hemp reinforcement ratio, their loads were averaged in a single value and the percent gain in out-of-plane capacity was computed. It is shown in Figure 4.15 that the hemp reinforcement ratio has a major effect on the flexural capacity gain of the masonry walls. For the HS series with a hemp reinforcement ratio of 0.381%, the strengthening system provided 80% increase in the flexural capacity of the wall compared to the control wall specimen. As the hemp reinforcement ratio increased from 0.381 to 1.2%, the gain in flexural capacity of the wall increased significantly from 80 to 320%. The increase in the hemp reinforcement ratio from 1.2 to 2.0% for the H3 series also resulted in an improvement in the flexural capacity of the wall which increased from 320 to 554%. However, adding more than 2 layers of hemp fiber fabric composites to increase the reinforcement ratio would decrease the effectiveness of this strengthening technique in enhancing the flexural capacity of unreinforced masonry walls. Using a reinforcement ratio greater than 2.0% will result in significant reduction in the utilization of hemp fiber fabric composites.

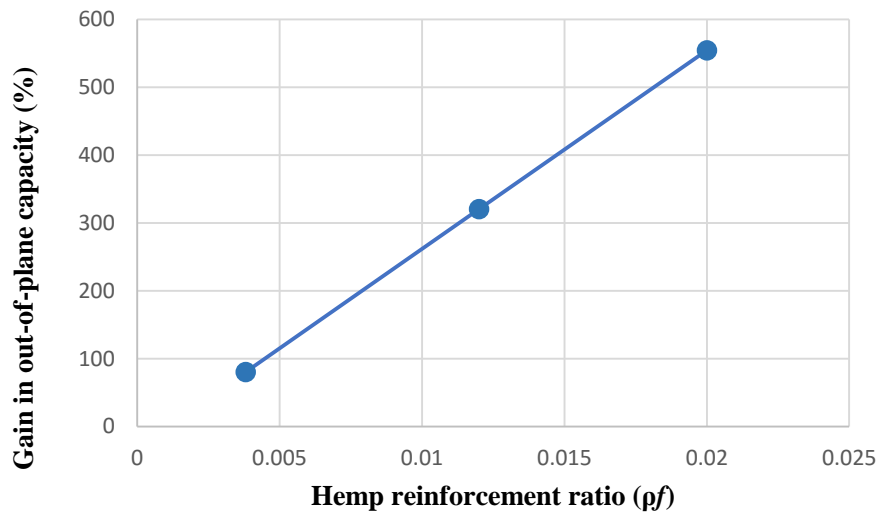


Figure 4.15 Gain in Out-of-Plane Capacity of Strengthened Walls.

4.3.2. Ductility Index

Ductility of a structural member can be defined as its ability to sustain large inelastic deformations before failure without substantial reduction in strength. Ductility is the inelastic deformation capacity. It is a function of material response and the structural member's response. Ductility is an essential requirement for earthquake resistant structures. Ductility provides a warning of failure to occupants of the structure and provides sufficient time for taking preventive measures.

In reinforced concrete structures, ductility is provided by the yielding of steel reinforcement that has a high tensile strength. Deflection ductility in reinforced concrete members is defined as the ratio of ultimate to yield deformation and it determines if the member has adequate ductility or not. However, for hemp-reinforced members, the definition of ductility is different and is not related to reinforcement yield point. Hemp fibers behave differently than steel fibers. As shown in Figure 3.10, hemp fibers are elastic up to failure and lack the yielding characteristics of steel fibers.

To evaluate the ductility of the hemp-reinforced walls, a method based on the fracture energy, or absorbed energy, was used. Fracture energy is defined as the amount of energy absorbed by the specimen until it breaks. Having the load-deflection response, the total absorbed energy by the wall, its fracture energy, is simply given by the area under the curve. To compare the performance of the strengthened walls to the control wall, the fracture energies of the strengthened walls are compared to the fracture energy of the control wall using a ductility index. The ductility index is a ratio of the fracture energy of a strengthened wall to the fracture energy of the unstrengthened wall.

$$Ductility\ Index = \frac{Fracture\ energy\ of\ strengthened\ wall}{Fracture\ energy\ of\ unstrengthened\ wall} \quad (8)$$

Table 4.1 shows the fracture energies and ductility indices of each series of walls. The ductility indices of the walls are plotted against the reinforcement ratios, shown in Figure 4.16. As series H1 and H2 have the same hemp reinforcement ratio, their ductility indices were averaged in a single value as shown in the curve. In all of the wall series, significant enhancement in ductility is noticed. The ductility index increases with the increase of the reinforcement ratio. This indicates that the higher the reinforcement ratio the more energy is absorbed by the specimen and more energy is needed to damage the specimen and rupture the hemp reinforcement layer. This result confirms that the strengthening method used was effective in increasing the energy absorption as well as the ductility of the hemp-reinforced walls.

Table 4.1 Fracture Energy and Ductility Index of the Wall Specimens.

Series	Reinforcement Ratio (%)	Fracture Energy (Nm)	Ductility Index
Control	--	0.5514	1
H S	0.381	12.625	22.89
H 1	1.2	162.25	294.25
H 2	1.2	326.48	592.1
H 3	2.0	1,014.1	1,839.1

Although series H1 and H2 have the same reinforcement ratio, series H2 resulted in an increased ultimate midspan deflection. Thus, the area under the load-deflection curve was larger than series H1 which explains the larger ductility index of series H2. Series H2 showed greater ductility due to the anchors provided at the ends of the wall. The gradual loss of bond between the anchors and the masonry before rupture of the hemp reinforcement resulted in a less brittle ultimate response and a slightly lower flexural capacity. It should be noted that adding more layers of hemp fiber fabric composites to increase the reinforcement ratio would decrease the effectiveness of this strengthening technique in enhancing the ductility of unreinforced masonry walls. Using a reinforcement ratio greater than 2.0% will result in significant reduction in the utilization of hemp fiber fabric composites and the strengthened wall loses its ductile behavior.

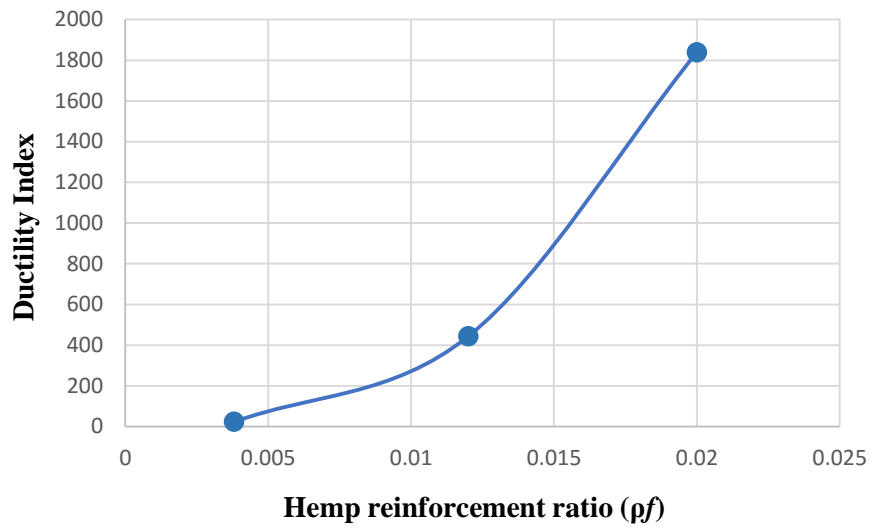


Figure 4.16 Effect of Hemp Reinforcement Ratio on the Ductility Index.

4.4. Failure Modes

In this section, the failure modes of individual wall specimens will be presented. Failure of the wall specimen is defined here as the point when the wall can no longer accommodate any increase in load.



Figure 4.17 Failure Mode of Control Wall C1.

Three modes of failure were observed from all the nine wall specimens tested. The three modes of failure are: flexural failure, shear failure, and rupture of the fiber reinforcement. No failure due to debonding between the hemp fiber reinforcement and the masonry units was observed in any of the wall specimens. Table 4.2 summarizes the failure modes of each series along with the corresponding average failure load and ultimate midspan deflection. The failure modes of all strengthened specimens as well as a typical deflected shape and crack patterns are shown in Figure 4.19 to 4.22.

Table 4.2 Summary of Experimental Results for Walls Tested in this Study.

Series Name	Ultimate Load (kN)	Ultimate Midspan Deflection (mm)	Failure Mode
C	2.49	-0.4015	Flexural Failure
H S	4.49	-4.162	Hemp Rupture
H 1	10.72	-16.47	Hemp Rupture
H 2	10.22	-37.47	Hemp Rupture
H 3	16.3	-73.68	Shear Failure



Figure 4.18 Failure Mode of H1-a.



Figure 4.19 Failure Mode of H1-a (vertical view).

For the unstrengthened specimen C1, the failure of the wall initiated near the two line loads with the appearance of cracks in the mortar head joints that propagated along the width of the wall. The cracks increased with the increase of the load which lead to a sudden failure of the wall at 2 locations, as shown in Figure 4.17. The failure of the control wall specimen occurred at a very low load, approximately 2.5 kN, and the measured midspan deflection was only 0.6 mm.



Figure 4.20 Failure Mode of H1-b.



Figure 4.21 Failure Mode of H1-b (vertical view).

For series (H1), wall specimen H1-a failed at the maximum moment region due to the rupture of the hemp reinforcement after the development of flexural cracks located at the mortar head joints near the load line. The maximum load measured was 11 kN and the midspan deflection measured was 16.5 mm before it failed suddenly. Wall specimen H1-b failed in a similar manner as wall specimen H1-a and at the same location as well at a maximum load of 10.44 kN. However, the midspan deflection measured was 6.6 mm.



Figure 4.22 Failure Mode of H2-a.

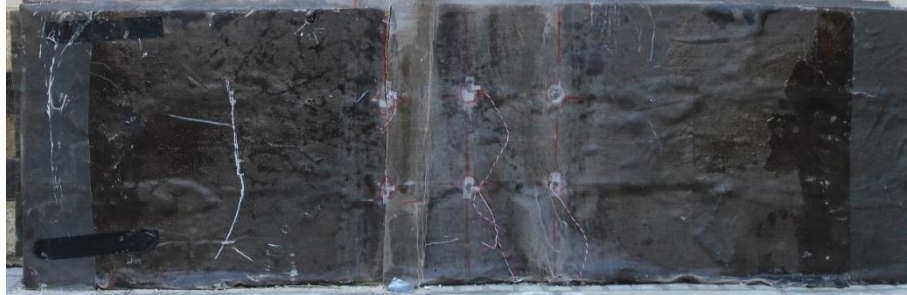


Figure 4.23 Failure Mode of H2-a (vertical view).

For series (H2), the failure of the wall specimen H2-a initiated by the development of microcracks in the masonry-mortar interface. As the load increased, cracks started to become visible in the mortar head joints that propagated along the width and the wall failed at the maximum moment region due to the rupture of the hemp reinforcement. The maximum load measured was 9.04 kN and the midspan deflection measured was 37.5 mm before it failed suddenly.



Figure 4.24 Failure Mode of H2-b.



Figure 4.25 Failure Mode of H2-b (vertical view).

Wall specimen H2-b failed in a similar manner as wall specimen H2-a and at the same location as well at a maximum load of 11.34 kN and the midspan deflection measured was 36.5 mm. In all of the walls of series H1 and H2 the specimens' failure occurred without significant warning. This brittle failure mode of the specimens was expected since the stress-strain behavior of the hemp fabric material used as the reinforcement lacks any form of yielding that is typically associated with standard steel reinforcement.

Shear failure governed the wall specimens in series (H3) as both specimens, H3-a and H3-a, failed in shear. The failure of both specimens initiated by the development of microcracks in the masonry-mortar interface. As the load increased, a series of flexural cracks started to become visible in the mortar head and bed joints that propagated along the width of the wall concentrated at the maximum moment region. Shear failure in the blocks initiated underneath both loading points at the top of the wall and extended to the bottom side causing local debonding of the hemp reinforcement. The hemp reinforcement did not rupture nor did it debond anywhere else along the walls. The maximum loads measured were 17.56 kN and 14.59 kN, and the midspan deflections measured were 57.3 mm and 73.7 mm for walls H3-a and H3-b, respectively.

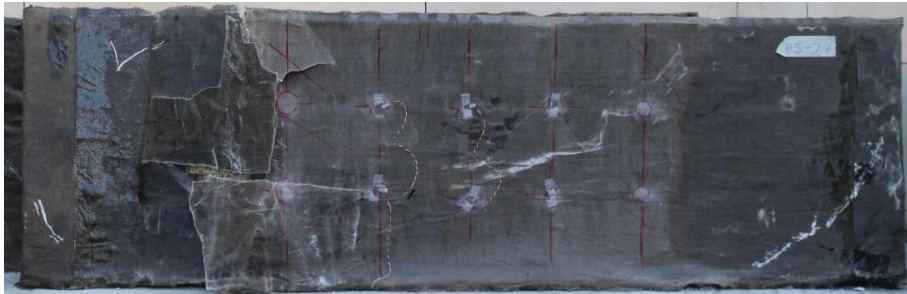


Figure 4.26 Failure Mode of H3-a.

In this type of failure, the hemp fiber fabric did not reach its ultimate tensile strength due to the high reinforcement ratio of the walls of series H3. This resulted in keeping the hemp fiber fabric intact and prevented it from rupturing while the masonry blocks of the walls reached their ultimate strength and failed in shear.



Figure 4.27 Failure Mode of H3-b.

Figure 4.29 presents a schematic view of the typical crack patterns developed on a wall specimen from series H3. The schematic shows the failure plane in the masonry unit in which the wall failure occurred. As for series (HS), wall specimen HS-b failed at midspan due the development of flexural cracks that lead to the rupture of the hemp reinforcement at a maximum load of 4.49 kN and a midspan deflection of 4.2 mm.



Figure 4.28 Deflected Shape of Wall H3-b.

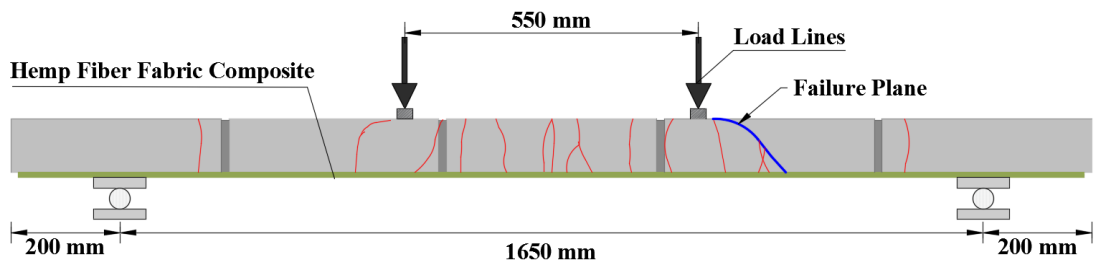


Figure 4.29 Schematic View of Series H3 Cracked Wall Specimen.



Figure 4.30 Failure Mode of HS-b.

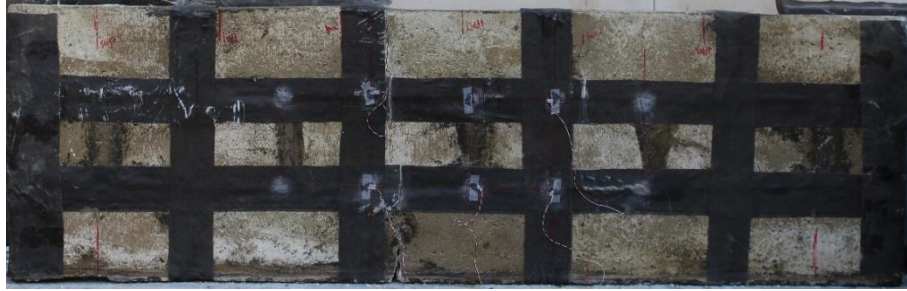


Figure 4.31 Failure Mode of HS-b (vertical view).

4.5. Performance of Analytical Model

Analytical load carrying capacities of the control and strengthened specimens are computed using the proposed methods in section 3.3.4. In this study, the section analysis procedure was followed to calculate the out-of-plane capacity of both unstrengthened and hemp fiber fabric-strengthened URM walls.

4.5.1. Unstrengthened Walls

The ultimate moment capacity of the unstrengthened control wall specimen was computed using Equation (2). In this study, masonry's modulus of rupture f'_r is assumed to be 10% of the minimum compressive strength, f'_m , obtained for mortar cubes, individual masonry units, and masonry prisms. The minimum value of compressive strength obtained was the average value of the masonry prisms with $f'_m=11.2$ MPa. Also, the ultimate moment capacity of the unstrengthened control wall specimen was computed using the Masonry Standards Joint Committee (MSJC 2013) and the result was compared to the proposed method. According to Section 9.1.9.2 of the MSJC code (MSJC 2013), the modulus of rupture, f_r , for masonry elements subjected to out-of-plane or in-plane bending shall be in accordance with the values in

Table 9.1.9.2. According to this table, the masonry's modulus of rupture is taken to be 1.149 MPa for hollow ungrouted masonry with the direction of flexural stress parallel to bed joints in running bond. The moment capacity was calculated using both moduli and ultimate load results are shown in Table 4.3. Both the proposed and the MSJC methods underestimate the ultimate load capacity of the unstrengthened wall by 16 % and 13%, respectively. However, both methods present a good and conservative estimate of the ultimate load capacity.

Table 4.3 Experimental and Analytical Results for Unstrengthened Wall.

Wall Identifier	Experimental	Proposed	MSJC (2013)	Experimental/ Proposed	Experimental/ MSJC
C1	2.49	2.14	2.19	1.16	1.13

4.5.2. Hemp-Strengthened Walls

The ultimate moment capacity of the strengthened walls was computed using the proposed method presented in section 1.1.1.2.1 of this study. Equation (7) was used to compute the ultimate moment capacity for each series and the ultimate load was calculated and compared with the experimental ultimate load. It should be noted that the computation of the ultimate capacities of the specimens did not include or consider the effect of the hemp anchorages on the ultimate capacity. Also, for series HS, the computation of the ultimate capacity included only the contribution of the hemp strips bonded parallel to the direction of bending and the effects of hemp strips bonded perpendicular to the direction of bending were ignored. Average analytical capacities were found to be 6.8% lower than the experimental capacities. The proposed method for computing the ultimate capacities of the strengthened specimens resulted in 38, 8.3, 3.3,

and 2.5% lower capacities than the experimental capacities for series HS, H1, H2, and H3, respectively. The ratios of the experimental to proposed ultimate capacity are presented in Table 4.4. It is evident from Table 4.4 that the proposed model provides a good estimate of the load capacities of the hemp strengthened walls. Figure 4.32 compares the experimental to predicted ultimate failure loads for all specimens and shows that the predicted failures of strengthened and unstrengthened walls are conservative.

Table 4.4 Experimental and Analytical Results for Hemp Strengthened Walls.

Series Name	Experimental Ultimate Load (kN)	Proposed Ultimate Load (kN)	Experimental/Proposed
H S	4.49	3.26	1.37
H 1	10.72	9.90	1.08
H 2	10.22	9.90	1.03
H 3	16.3	15.91	1.02

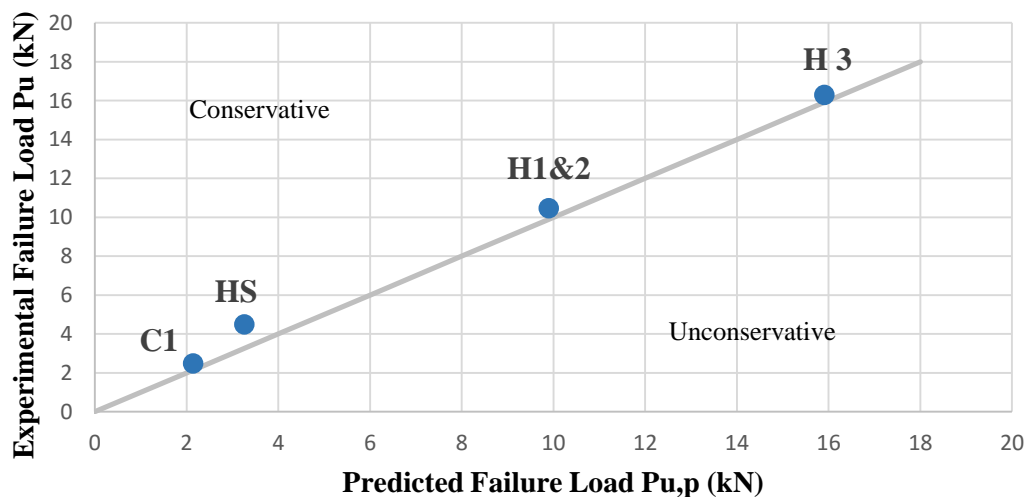


Figure 4.32 Experimental Failure Load to Predicted Load Results.

CHAPTER 5

SUMMARY, CONCLUSIONS, AND RECOMMENDATIONS

5.1. Research Summary

A large percentage of existing buildings around the world have been constructed with unreinforced masonry. These buildings are threatened to collapse during earthquakes, which imposes high safety risks. A literature review showed that retrofitting jobs of structures have been limited to the use of composites made from synthetic material such as carbon, glass or aramid fibers, etc. The existing knowledge in improving structures, including masonry walls, using natural fibers, is hardly applied. Lack of knowledge about out-of-plane capacity of URM walls strengthened with natural fibers led to the development of an experimental program presented in this thesis.

In this study, the feasibility of the use of hemp fiber fabric composite to strengthen unreinforced masonry walls against out-of-plane loads has been investigated. A total of eight masonry wall specimens were tested in the out-of-plane direction using two line loads placed at one third the length of the span from the supports. The wall specimens were 2.05 m long, 0.63 m wide, and 0.10 m deep. Out of the total eight walls tested, seven walls were strengthened with hemp fiber fabric of different configurations. The parameters investigated were the amount of reinforcement layers and the anchorage of the hemp reinforcement. The load-deflection curves of each specimen were recorded for each test. The ultimate moment capacity of the unstrengthened walls was estimated using a simple analytical approach. A proposed analytical model was used to determine the out-of-plane capacity of the hemp-strengthened walls and results were compared to the experimental results.

5.2. Research Conclusions

Based on the experimental and analytical results presented in this research, the following conclusions can be drawn:

- 1- The overall response of the strengthened walls was similar and can be divided into two phases. The first phase of the response is almost linear and characterizes the stiffness contribution of the masonry components of the walls. The second phase of the response is a non-linear stage which characterizes the stiffness contribution from the hemp fiber reinforcement. This portion of the load-deflection curve signifies the role of the hemp fiber reinforcement to the performance of the specimen.
- 2- Externally bonded hemp fiber fabric composite systems significantly enhance the load carrying capacity of unreinforced masonry walls subjected to out-of-plane loads. As the hemp reinforcement ratio increases, the flexural capacity of the walls also increases. The increase in hemp reinforcement ratio to 2.0% enhanced the load carrying capacity of the walls greatly with up to 554% gain in out-of-plane capacity compared to the control unreinforced specimen.
- 3- The hemp fiber fabric composites significantly increase the out-of-plane deflection capacity of unreinforced masonry walls. As the hemp reinforcement ratio increases, the ductility of the walls also increases. The ductility is measured by the fracture energy of the specimens. Thus, an increase in the ductility leads to an increase in the energy absorption capacity. The strengthening method used was effective in increasing the energy absorption as well as the ductility of the hemp-reinforced walls.

- 4- Rupture of the hemp fiber reinforcement was the most common mode of failure of the strengthened specimens. Failure initiated by the development of microcracks in the masonry-mortar interface and as the load increased, cracks started to become visible in the mortar head joints that propagated along the width and the wall failed at the maximum moment region.
- 5- Shear failure governed the wall specimens strengthened with a reinforcement ratio of 2.0%. The hemp fiber fabric composite did not reach its ultimate tensile strength due to the high reinforcement ratio of the walls. This prevented the hemp fibers from rupturing while the masonry blocks of the walls reached their ultimate strength and failed in shear.
- 6- Adding more layers of hemp fiber fabric composites to increase the reinforcement ratio would decrease the effectiveness of this strengthening technique in enhancing the flexural capacity and ductility of unreinforced masonry walls. Using a reinforcement ratio greater than 2.0% will result in significant reduction in the utilization of hemp fiber fabric composites and the strengthened wall loses its ductile behavior.
- 7- In this study, an analytical model was proposed for unstrengthened and strengthened walls. A comparison of the model prediction with the experimental results shows that the proposed model underestimates the ultimate load capacity of the unstrengthened wall by 16 %. Average analytical capacities are found to be approximately 6.8% lower than the experimental capacities for strengthened specimens. The predicted ultimate load carrying capacities of strengthened and unstrengthened walls are considered conservative.

5.3. Research Recommendations

Based on the promising results of this experimental study of strengthening unreinforced masonry using natural fibers, further research is recommended to:

- 1- Perform out-of-plane testing on bigger scale walls strengthened with hemp fiber fabric composites.
- 2- Validate the analytical model in a statistically significant manner by testing additional wall specimens strengthened with hemp fiber fabric composites in the out-of-plane direction.
- 3- Investigate the in-plane seismic behavior and failure modes of walls strengthened with hemp fiber fabric composites.
- 4- Investigate the long-term durability of the bond of the strengthening system.

REFERENCES

- Abdo, M. A., & Hori, M. (2012). Reliability of Using 3D woven Polypropylene Fiber in Strengthening of a Large-Scale RC Structure Subjected to Seismic Loads. *Arabian Journal for Science and Engineering*, 37(3).
- American Concrete Institute, ACI Committee 440. (2010). *Guide for the Design and Construction of Externally Bonded FRP Systems for Strengthening Concrete Structures*. Detroit, Michigan.
- American Society for Testing and Materials. (2010). Standard test methods for compressive strength of cylindrical concrete specimens. *ASTM C39*.
- American Society for Testing and Materials. (2011). Standard Specification for Tensile Testing Machines for Textiles. *ASTM D76*.
- American Society for Testing and Materials. (2014). Standard Test Method for Tensile Properties of Single Textile Fibers. *ASTM D3822*.
- American Society for Testing and Materials. (2015). Standard Test Methods for Flexural Bond Strength of Masonry. *ASTM E518*.
- Awwad, E. A. (2011). *Sustainable building systems: Alternative construction materials (Doctoral dissertation)*. Beirut: American University of Beirut, Department of Civil and Environmental Engineering.
- Bauccio, M. (1994). *Engineering materials reference book*, 2nd ed. *ASM International*. Ohio.

- Beckermann, G. a. (2008). Engineering and evaluation of hemp fiber reinforced polypropylene composites: Fibre treatment and matrix modification. *ournal of Composites Part A-Applied Science*, 39, 979–988.
- Berglund, L. (2006). New concepts in natural fiber composites. *Proceedings of the 27th Riso International Symposium on Materials Science: Polymer Composite Materials for Wind Power Turbines*. Roskilde, Denmark.
- Bischof, P., & Suter, R. (2014). Retrofitting Masonry Walls with Carbon Mesh. *Journal of Polymers*, 6, 280-299.
- Bledzki, A., Fink, H., & Specht, K. (2004). bidirectional hemp and flax EP- and PP-composites: Influence of defined fiber treatments. *Journal of Applied Polymer Science*, 93, 2150–2156.
- Bledzki, A., Reihmane, S., & Gassan, J. (1996). Properties and modification methods for vegetable fibers for natural fiber composites. *Journal of Applied Polymer Science*, 59, 1329–1336.
- Bogoeva-Gaceva et al., G. A. (2007). Natural fiber eco composites. *Polymer Composite Journal*, 28, 98–107.
- Bolton, A. (1995). The potential of crop fibers as crops for industrial use. *Outlook Agriculture*, 24, 85–89.
- Bournas, D., & Triantafillou, T. (2009). Flexural strengthening of RC columns with NSM FRP or stainless steel. *Structural Journal*, 106(4), 495–505.
- Brouwer, W. (2000). Natural fiber composites - From upholstery to structural components. *Natural Fibres for Automotive Industry Conference*. Manchester, UK.

- Carus, M., & ScholZ, L. (2011). *Targets for bio-based composites and natural fibres*. Biowerkstoff Report.
- Catling, D. (1982). *Identification of Vegetable Fibres*. London: Springer Netherlands.
- ElGawady, M., Lestuzzi, P., & Badoux, M. (2006). Aseismic retrofitting of unreinforced masonry walls using FRP. *Journal of Composites: Part B*, 37, 148–162.
- Hamoush et al., S. A. (2001). Out-Of-Plane Strengthening Of Masonry Walls With Reinforced Composites. *Journal of Composites for Construction*, 5(3).
- Ivens, J., Bos, H., & Verpoest, I. (1997). The applicability of natural fibers as reinforcement for polymer composites. *Industrial Outlets and Research for 21st Century*. Wageningen, The Netherlands.
- Jarman, C. (1998). Plant Fibre processing (Small scale textile series). 64.
- Kalali, A., & Kabir, M. Z. (n.d.). Cyclic behavior of perforated masonry walls strengthened with glass fiber reinforced polymers. *Scientia Iranica A*, 19(2), 151–165.
- Li et al., G. Q. (2005). Experimental study of FRP tube-encased concrete columns. *Journal of Composite Materials*, 39, 1131-1140.
- Liu et al., Q. S. (2007). Structural bio-composites from flax – part II: the use of PEG and PVA as interfacial compatiblising agents. *Journal of Composites Part A*, 38, 1403-1413.
- Menna et al., C. A. (2015). Structural behaviour of masonry panels strengthened with an innovative hemp fibre composite grid. *Journal of Construction and Building Materials*, 100, 111–121.
- Mougin, G. (2006). Natural fiber composites - problems and solutions. *JEC Composite*, 25, 32–35.

- MSJC (Masonry Standards Joint Committee). (2013). Building Code Requirements for Masonry Structures. *TMS 402/ACI 530/ASCE 6*.
- Mueller, D., & Krobjilowski, A. (2003). New discovery in the properties of composites reinforced with natural fibers. *Journal of Industrial Textiles*, 33, 111–130.
- Netravali, A., & Chabba, S. (2003). Composites get greener. *Materials Today*, 6, 22–29.
- Nishino, T. (2004). Natural fiber sources. In C. Baille, *Green Composites: Polymer Composites and the Environment* (pp. 49–80). Cambridge: Woodhead Publishing Limited.
- Olesen, P., & Plackett, D. (1999). Perspectives on the performance of natural plant fibers. *Natural Fibres Performance Forum - Plant Fibre Products - Essentials for the Future*. Copenhagen, Denmark.
- Pampanin, S. (2006). Controversial Aspects in Seismic Assessment and Retrofit of Structures in Modern Times: Understanding and Implementing Lessons from Ancient Heritage. *Bulletin of the New Zealand Society for Earthquake Engineering*, 39(2).
- Papanicolaou, C., Triantafillou, T., & Lekka, M. (2011). Externally bonded grids as strengthening and seismic retrofitting materials of masonry panels. *Construction and Building Materials Journal*, 25(2), 504–514.
- Papanicolaou, C., Triantafillou, T., Karlos, K., & Papathanasiou, M. (2007). Textile-reinforced mortar (TRM) versus FRP as strengthening material of URM walls: in-plane cyclic loading. *Journal of Material and Structures*, 40(10), 1081–1090.
- Papanicolaou, C., Triantafillou, T., Karlos, K., & Papathanasiou, M. (2008). Textile-reinforced mortar (TRM) versus FRP as strengthening material of URM walls: out-of-plane cyclic loading. *Journal of Material and Structures*, 41(1), 143–157.

- Prota, Marcari, G., Fabbrocino, G., Manfredi, G., & Aldea, C. (2006). Experimental in-plane behavior of tuff masonry strengthened with cementitious matrix–grid composites. *Journal of Composite Construction*, 10(3), 223–233.
- Reitherman, R., & Perry, C. (2009). Unreinforced Masonry Buildings and Earthquakes. FEMA. Retrieved from <http://www.fema.gov/media-library-data/20130726-1728-25045-2959/femap774.pdf>
- Santa-Maria, H., & Alcaino, P. (n.d.). Repair of in-plane shear damaged masonry walls with external FRP. *Journal of Construction and Building Materials*, 25, 1172–1180.
- Sedan et al., D. P. (2008). Mechanical Properties of Hemp Fibre Reinforced Cement: Influence of the Fibre/Matrix Interaction. *Journal of the European Ceramic Society*, 28, 183–192.
- Sen, T., & Reddy, H. (2011). A Numerical Study of Strengthening of RCC Beam Using Natural Bamboo Fibre. *International Journal of Computer Theory and Engineering*, 3(5).
- Sen, T., & Reddy, H. (2011). Application of Sisal, Bamboo, Coir and Jute Natural Composites in Structural Upgradation. *International Journal of Innovation, Management and Technology*, 2(3).
- Sen, T., & Reddy, H. (2011). Finite Element Simulation of Retrofitting of RCC Beam Using Coir Fibre Composite. *International Journal of Innovation, Management and Technology*, 2(2).
- Shahzad, A. (2011). Hemp fiber and its composites – a review. *Journal of Composite Materials*, 46(8), 973–986.

- Symington, M., Banks, W., West, O., & Pethrick, R. (2009). Tensile Testing of Cellulose Based Natural Fibers for Structural Composite Applications. *Journal of Composite Materials*, 43(9).
- Tan, K. H., & Patoary, M. K. (2004). Strengthening of Masonry Walls against Out-of Plane Loads Using Fiber-Reinforced Polymer Reinforcement. *Journal of Composites for Construction*, 8(1).
- Triantafillou, T. (n.d.). A New Generation of Composite Materials as Alternative to Fibre-reinforced Polymers (FRP) for Strengthening and Seismic Retrofitting of Structures.
- Triantafillou, T., & Papanicolaou, C. (2006). Shear strengthening of reinforced concrete members with textile reinforced mortar (TRM) jackets. *Journal of Material and Structures*, 39(1), 93–103.
- Triantafillou, T., Papanicolaou, C., Zissimopoulos, P., & Laourdekis, T. (2006). Concrete confinement with textile-reinforced mortar jackets. *Journal of Structures*, 103(1), 28–37.
- Wang, B., Sain, M., & Oksman, K. (2007). Study of structural morphology of hemp fiber from the micro to the nanoscale. *Applied Composite Materials*, 14, 89–103.
- Yan, L., & Chouw, N. (2012). Behavior and analytical modeling of natural flax fibre-reinforced polymer tube confined plain concrete and coir fibre-reinforced concrete. *Journal of Composite Materials*, 47(17), 2133–2148.
- Yan, L., & Chouw, N. (2013). Compressive and flexural behaviour and theoretical analysis of flax fibre reinforced polymer tube encased coir fibre reinforced concrete composite. *Materials and Design*, 52, 801–811.

- Yan, L., & Chouw, N. (2013). Experimental study of flax FRP tube encased coir fibre reinforced concrete composite column. *Construction and Building Materials Journal*, 40, 1118–1127.
- Yan, L., & Chouw, N. (2014). Natural FRP tube confined fibre reinforced concrete under pure axial compression: A comparison with glass/carbon FRP. *Journal of Thin-Walled Structures*, 82, 159–169.
- Yan, L., Chouw, N., & Jayaraman, K. (2013). Compressive and Flexural Behavior of Natural Flax FRP Tube Confined Coir Fiber Reinforced Concrete. *FRPRCS11*.
- Yan, L., Chouw, N., & Jayaraman, K. (2014). Effect of column parameters on flax FRP confined coir fibre reinforced concrete. *Construction and Building Materials Journal*, 55, 299–312.
- Yan, L., Chouw, N., Yuan, X., & Nguyen, C. (2012). Compressive Behaviour of Flax Frp Tube Confined Coir Fibre Reinforced Concrete. *BEFIB 2012*.
- Zhu, Z., Ahmad, I., & Mirmiran, A. (2005). Effect of column parameters on axial compression behavior of concrete-filled FRP tubes. *Advanced Structural Engineering*, 8, 443–449.
- Zohrevand, P., & Mirmiran, A. (2011). Behaviour of ultra-high performance concrete confined by fibre reinforced polymers. *Journal of Materials in Civil Engineering*, 23, 1727-1734.